

FINAL REPORT

SPACE SHUTTLE MAIN ENGINE STRUCTURAL ANALYSIS AND DATA REDUCTION/EVALUATION

VOLUME 3A: HIGH PRESSURE OXIDIZER TURBO-PUMP PREBURNER PUMP HOUSING STRESS ANALYSIS REPORT

April 1989

Contract NAS8-37282

Prepared for

NATIONAL AERONAUTICS AND SPACE ADMINISTRATION
GEORGE C. MARSHALL SPACE FLIGHT CENTER, AL 35812

by

Robert V. Shannon, Jr.

 **Lockheed**
Missiles & Space Company, Inc.
Huntsville Engineering Center
4800 Bradford Blvd., Huntsville, AL 35807

ORIGINAL CONTAINS
COLOR ILLUSTRATIONS

(NASA-CR-183665) SPACE SHUTTLE MAIN ENGINE
STRUCTURAL ANALYSIS AND DATA
REDUCTION/EVALUATION, VOLUME 3A: HIGH
PRESSURE OXIDIZER TURBO-PUMP PREBURNER PUMP
HOUSING STRESS ANALYSIS REPORT (Lockheed)

M89-27694

G3/20 Unclass
0211796

FINAL REPORT

**SPACE SHUTTLE MAIN ENGINE STRUCTURAL
ANALYSIS AND DATA REDUCTION/EVALUATION**

**VOLUME 3A: HIGH PRESSURE OXIDIZER TURBO-PUMP
PREBURNER PUMP HOUSING STRESS
ANALYSIS REPORT**

April 1989

Contract NAS8-37282

Prepared for

**NATIONAL AERONAUTICS AND SPACE ADMINISTRATION
GEORGE C. MARSHALL SPACE FLIGHT CENTER, AL 35812**

by

Robert V. Shannon, Jr.

**LOCKHEED-HUNTSVILLE ENGINEERING CENTER
4800 Bradford Boulevard
Huntsville, AL 35807**

Appendix A
IBM AND CRAY RUNSTREAMS

APPENDIX A

IBM RUNSTREAM

EDIT ---- CRVS202.HPOTP.GEN(IBMJCL)

```
***** TOP OF DATA *****
000001 //CRVS202 JOB (6ED554590417),'SHANNON',NOTIFY=CRVS202,CLASS=A,
000002 // MSGCLASS=X
000003 //DELETE EXEC PGM=IEFBR14
000004 //F1 DD DISP=(MOD,DELETE),UNIT=SYSDA,
000005 // SPACE=(TRK,(1)),DSN=CRVS202.ANSYS.HPOTP.FILE27
000006 // *
000007 //ANSYS43 EXEC ANSYS43,C=CATLG,
000008 // F27='CRVS202.ANSYS.HPOTP.FILE27'
000009 //GO.FILE27 DD SPACE=(4652,(9000,500),RLSE),
000010 // DISP=(NEW,CATLG),UNIT=(SYSDA,8)
000011 //*O.FILE28 DD DSN=CRVS202.ANSYS.HPOTP.FILE28,
000012 // * DCB=(RECFM=FB,LRECL=80,BLKSIZE=400),DISP=(OLD,KEEP)
000013 //GO.FT05F001 DD DSN=CRVS202.HPOTP.GEN(HPOTP7),
000014 // SPACE=(4096,(9000,1500),RLSE),DISP=SHR
000015 //
***** BOTTOM OF DATA *****
```

CRAY RUNSTREAM

EDIT ---- CRVS202.HPOTP.GEN(CRAYJCL)

```
***** TOP OF DATA *****
000001 JOB,JN=CRVS202,MFL=6000000,T=6000,OLM=8000,SSD=50000.
000002 ACCOUNT,AC=6ED554590417,US=CRVS202.
000003 OPTION,STAT.
000004 FETCH,DN=FT27,TEXT='DSN=CRVS202.ANSYS.HPOTP.FILE27'.
000005 ACCESS,DN=ANSYS,PDN=SOL43N,ID=ANSYS43,OWN=SYSTEM.
000006 ASSIGN,DN=FT11,LM=400000,BS=24,DV=SSD-0-20.
000007 ACCESS,DN=AUTH43,ID=ANSYS43,OWN=SYSTEM. ACCESS AUTHORIZATION FILE
000008 MODE,BT=DISABLE.
000009 ANSYS.
000010 SAVE,DN=FT14,PDN=HPOT14.
000011 DISPOSE,DN=FT14,DC=ST,TEXT='DSN=CRVS202.ANSYS.HPOTP.FILE14,^
000012         'DISP=(,CATLG),'^
000013         'SPACE=(CYL,(120,20),RLSE),'^
000014         'DCB=(RECFM=FB,BLKSIZE=6320,LRECL=80)',WAIT.
000015 /EOF
000016 /CORE,5.7E6
000017 /INPUT,27
000018 FINISH
000019 /AUX1
000020 BCDCNV
000021 FINISH
***** BOTTOM OF DATA *****
```


FOREWORD

This volume of the final report summarizes the model generation and structural analysis performed for the high pressure oxidizer turbo-pump (HPOTP) preburner pump volute housing located on the main pump end of the HPOTP in the Space Shuttle Main Engine. An ANSYS finite element model of the volute housing was built and executed by Robert V. Shannon, Jr., and Mark D. Stansberry of the Structures & Mechanics Group at the Lockheed-Huntsville Engineering Center under NASA Contract NAS8-37282. A static structural analysis was performed on the Marshall Space Flight Center (MSFC) Engineering Analysis and Data System (EADS) Cray-XMP supercomputer.

CONTENTS

<u>Section</u>		<u>Page</u>
	FOREWORD	ii
1	INTRODUCTION AND OVERVIEW	1
2	MODEL DESCRIPTION	3
3	BOUNDARY CONDITIONS AND EXTERNAL LOADS	7
4	MATERIAL PROPERTIES	9
5	STRUCTURAL ANALYSIS/RESULTS	10
6	SUMMARY	12
7	RECOMMENDATIONS	13
8	REFERENCES	15

Appendix

A	IBM and Cray Runstreams	A-1
---	-------------------------	-----

LIST OF TABLES

<u>Table</u>		<u>Page</u>
1	Element Material and Type Numbers for Global Element Regions	16
2	Element Material and Type Numbers for Elements Not in the Tongue Region	16
3	Element Material and Type Numbers for Elements in the Tongue Region	16
4	Node Angle Locations for Nodes from -25° to 147°, except on Discharge Pipe	17
5	Node Angle Locations for Nodes from 150° to -30°, except on Discharge Pipe	18
6	Numbering Scheme for Nodes from -21° to 147°, Except for Web and Flange Nodes	19

LIST OF TABLES (Concluded)

<u>Table</u>		<u>Page</u>
7	Numbering Scheme for Nodes from 150° to -75°, except for Web and Flange Nodes	20
8	Maximum Housing Von Mises Stresses	21
9	Maximum Housing Principal Stresses	21

LIST OF FIGURES

<u>Figure</u>		<u>Page</u>
1	Schematic of the HPOTP Major Components	22
2	Preburner Pump Housing and Preburner Pump Components	23
3	Preburner Pump Housing, View from Inlet Side	24
4	Cutaway View of Preburner Pump Housing	25
5	Orientation of Discharge Pipe with respect to Pump Housing Volute Passage	26
6	Overall Dimensions of the Preburner Pump Housing	27
7	Cross-Section Regions of the Model	28
8	Preburner Pump Housing Model Plot, View A from Inlet Side	29
9	Preburner Pump Housing Model Plot, View B from Inlet Side	30
10	Preburner Pump Housing Model, View from Main Pump Side	31
11	Cutaway View of Preburner Pump Housing Model	32
12	Diffuser Vane Elements	33
13	Two Preburner Pump Model Cross Sections 180° Apart	34
14	Pressure Loads and Boundary Conditions	35
15	INCONEL 718 Young's Modulus as a Function of Absolute Temperature (Rankine)	36
16	INCONEL 718 Poisson's Ratio as a Function of Absolute Temperature (Rankine)	36
17	Vanes Viewed from Inlet Side, Sigma -1 (Maximum Principal Stress)	37
18	Vanes Viewed from Inlet Side, Sigma -Z (Axial Stress)	38
19	Vanes Viewed from Inlet Side, Sigma -E (Von Mises Equivalent Stress)	39
20	Vanes Viewed from Pump Side, Sigma -1	40
21	Vanes Viewed from Pump Side, Sigma -Z	41
22	Vanes Viewed from Pump Side, Sigma -E	42
23	Sigma -1 for 68° to 76° Section	43
24	Sigma -E for 68° to 76° Section	44
25	Sigma -1 for 14° to 22° Section	45
26	Sigma -Z for 14° to 22° Section	46
27	Sigma -E for 14° to 22° Section	47

1. INTRODUCTION AND OVERVIEW

The high-pressure oxidizer turbo-pump (HPOTP) contains two single-stage centrifugal pumps on a common shaft which is driven directly by a two-stage hot-gas turbine. A schematic of the HPOTP major components can be seen in Figure 1. The HPOTP has overall dimensions of 24 by 36 in. and an approximate overall weight of 575 lb.

There are three main inlets and three main outlets in the HPOTP. The inlets are the main pump inlet, the preburner pump inlet, and the turbine inlet. The main fluid outlets are the main pump discharge, preburner pump discharge, and the turbine discharge. Liquid oxygen enters the main pump inlet from the low pressure oxidizer turbo-pump (LPOTP) and the main pump discharge supplies this oxygen to the LPOTP turbine, the heat exchanger, the preburner pump (via the preburner pump inlet duct, which is flange mounted to the preburner pump inlet), and the thrust chamber injector.

The preburner pump has a single entry impeller with four full blades and four partial blades. Figure 2 provides a closer view of the preburner pump region of the HPOTP. This figure shows how the preburner pump housing is flange mounted to the main pump housing. Figure 3 gives a view of the pump housing from the inlet side. The preburner pump discharge is evident in this figure. The impeller discharges oxidizer through the pump housing diffuser vanes and into the housing volute passage. The diffuser vanes cause a further rise in oxidizer pressure. Figure 4 is a cutaway view of the pump housing, exposing the volute passage and diffuser vanes. From the volute passage the oxidizer passes into the housing discharge pipe, where it then leaves the preburner pump housing. Figure 5 presents the orientation of the discharge pipe with respect to the preburner pump housing volute passage. Figure 6 shows a cross section of the preburner pump housing and provides this component's

overall dimensions. It is important to note that the preburner pump housing is a casting and, as such, contains no welds and is of one-piece construction.

The following sections of this report describe the preburner pump housing finite element model, boundary conditions and external loads, material properties, structural analysis and results, and the summary and recommendations.

2. MODEL DESCRIPTION

The global coordinate system used for the generation of this model is exactly the same as that used for the generation of the preburner pump bearing components. The origin of this system is at the radial symmetric center of the HPOTP turboshaft with the z-axis pointing towards the preburner pump inlet. The Cartesian x-axis lies at a station angle of 70.0° , relative to the preburner pump housing drawing (Ref. 1). The Cartesian y-axis is thus at a drawing station angle of 160.0° . The location of the global origin along the turboshaft is 0.052 in. toward the main pump from the main pump mating surface of the preburner pump housing flange. This flange is clearly identified in Figure 7, which presents the various regions of each model cross section. With respect to the dimensions (Figure 6), the smallest nodal z value is 0.052 in. and the z-value of the housing inlet mating surface is 4.102 in.

The finite element model of the preburner pump housing contains 15,694 brick and wedge elements, a total of 20,180 nodes, and 59,820 degrees of freedom. Maximum wavefront for solution of this model is about 2598. The ANSYS limit on model wavefronts is 3000. The plots in Figures 8 and 9 show the model when viewed from the inlet side of the housing, whereas Figure 10 is a view of the model from the main pump side of the preburner pump housing. The support bolt holes were not modeled in this final model due to the complexity caused by the diffuser vane geometry. Figure 11 shows the model when viewed from the inlet side with part of the model cut away to expose part of the vane region. Solid elements modeling the housing diffuser vanes are clearly evident. The stray elements in the foreground are part of the discharge pipe mesh. Finally, Figure 12 is simply a plot of the 11 housing diffuser vanes as they were modeled. Because of the odd number of vanes and the unusual circumferential spacing between them, no modeled vane is exactly like another modeled vane. In addition, all vanes have their noses and tails "clipped" due to overall modeling necessity.

A breakdown of the number of elements composing each major region of the model is given in Tables 1 through 3. Tables 2 and 3 refer to the "tongue region," which contains the volute tongue and the discharge pipe between global coordinate system angles -75° and -21° (i.e., blueprint station angles between -5° and 49°).

Tables 4 and 5 show the global cylindrical coordinate system angles for each of the 60 model stations. These tables show that nodes on the main pump side of the vanes are usually at slightly different circumferential coordinates than nodes on the inlet side of the vanes. This is to allow nodes on the main pump side to bracket the regions where the support housing bolt holes are drilled. Future versions of this model may include these bolt holes as an attempt to understand local stress interactions between the bolts, the bolt holes, and vane regions in the vicinity of the bolt holes. Some stations are marked in these tables with "b.c." which stands for "bolt center." These model stations correspond to locations where the support bolt holes are centered.

Tables 6 and 7 list node numbering for nodes between model station numbers 2 and 53. This node numbering scheme does not include nodes in the stiffening webs, in the discharge pipe, or in the preburner to main pump housing flange. It can be easily deduced from Tables 6 and 7 that there are 303 nodes per cross section (not including web and flange nodes) in this region of the model.

Nodes in the discharge pipe are numbered in the range 24,000 to 25,000. Nodes in the preburner to main pump housing flange are numbered from 20,000 to 20,359, for a total of 360 nodes. Rib nodes not in the tongue or discharge region are numbered between 24,000 and 24,958. Tongue passage nodes are numbered between 27,000 and 27,894.

Specific model information is provided in the preceding tables. The element type and material number information is useful for selecting a region of elements. Each model region has a different type and/or material number; therefore all the elements in a region may be selected by using one of the following ANSYS commands:

1. ESEL,TYPE,(TYPE NUMBER)
2. ESEL,MAT,(MATERIAL NUMBER)
3. ESEL,TYPE,(TYPE NUMBER)
ERSEL,MAT,(MATERIAL NUMBER)

For example, to create the plot of the diffuser vane elements in Figure 11, the vane elements were first selected out, using the commands

```
ESEL,TYPE,4
ERSEL,MAT,4
```

in accordance with the designation for the vanes in Table 1. Different material numbers are used for convenience only. The different material numbers are defined by exactly the same material property values. Listed below are two convenient coordinate systems whose z-axis runs down the discharge pipe axis. System 17 below is Cartesian and system 18 is a cylindrical system:

```
Local,17,0,1.180,-3.2419,2.952,21.00,-80.00,0.00
Local,18,1,1.180,-3.2419,2.952,21.00,-80.00,0.00
```

Figure 13 is a model plot that can be compared to Figure 6 (which was obtained from the housing drawing). The mesh shown for the two housing cross sections in Figure 13 is typical of other model cross sections.

It was decided that the support bolt holes would not be modeled for several reasons. First, further complexity in the model would probably require substructuring due to ANSYS wavefront limits or Cray supercomputer core memory limits. Second, an investigation into the interaction of the support bolt hole region stresses with the vane region stresses requires model detail greater than can be offered by this model. Third, the model is fairly complex in the vane region on the main pump side. The increase in overall model complexity created by modeling the support bolt holes outweighs the advantages gained by modeling them.

Appendix A lists the job control language used to create an ANSYS FILE27 (analysis file) from the ANSYS PREP7 deck on the MSFC EADS IBM 3084QX computer. Creation of the analysis file on the MSFC EADS IBM required approximately 101 minutes CPU time. Also included in Appendix A is a listing of the job control language used to create and save the ANSYS FILE14 (the binary solution file). The MSFC EADS Cray computer classified the run which created the FILE14 as a "HUGE2." Solution times on the Cray XMP were approximately 4000 seconds CPU.

3. BOUNDARY CONDITIONS AND EXTERNAL LOADS

All nodes on the housing flange surface facing the main pump were constrained in all degrees of freedom. This amounted to 240 constrained nodes. No other nodes were constrained from displacement; however, all nodes were constrained from rotations by the nature of the brick elements used in the model construction.

Figure 14 shows the applied pressures along with the axial load applied to the housing inlet. Internal applied pressures in the discharge pipe were 7000 psi. In all, there were 6207 applied element pressures and 1424 applied nodal forces. The applied nodal forces were due to axial loads placed on the inlet and discharge pipe flanges. Allowances were made to apply shear forces to these flanges using a small value (essentially zero) for the sake of the load case presented here.

No bolt loads were applied. Axial limit loads of 1950 lb and 530 lb were applied to the preburner pump inlet face and discharge pipe flange, respectively. Interference fit pressures caused by preburner pump bearing components were ignored relative to fluid pressures since the housing is far stiffer than the bearing components. No loads attributable to axial turboshaft motion were applied based on the assumption that the turboshaft is perfectly balanced.

Since only a first static analysis was performed, the results presented in this report do not include torque, shear, or moments acting on the preburner pump inlet or discharge pipe flange. Limit loads for the above neglected torque, moment, and shear loads can easily be applied for a subsequent static analysis.

No hot-fire strain gage or other data indicating fluid pressures acting on the housing vanes and passage were available. This lack of information forces the estimation of pressure acting in the vane and passage regions.

Accordingly, there is no difference between pressures applied to the suction and pressure sides of each vane. This condition is clearly unrealistic, but it is possible that analytical or empirical methods will be applied in the future to obtain estimates of the pressure differential across each diffuser vane. The format for applying the vane pressures allows for independently specifying pressures on the suction and pressure sides of the vanes should these pressures be determined. A large pressure differential could cause significant shear stress within a vane.

The loading condition applied to the preburner pump housing is a Full Power Level (FPL) load case of 7000 psi applied to the inside surface of the discharge pipe, the passage, the vanes, and the housing surfaces facing the impeller. Pressures applied to the inside surface of the housing inlet (4750 psi) also corresponded to FPL conditions.

In order to have the capability of running a static stress analysis at any practical ambient temperature, material properties were input as functions of temperature and then all nodal temperatures set to a uniform value. The load case presented in this report was applied at a uniform temperature of 210 °R (-250 °F).

4. MATERIAL PROPERTIES

The HPOTP preburner pump housing is constructed of cast INCONEL 718 heat treated in accordance with RB0170-155. The housing drawing allows for standard grade to be used in the inlet region, whereas critical grade criteria must be met everywhere else (see Figure 4). All material property information was obtained from the Rocketdyne Materials Properties Manual, except for data on the yield and ultimate strengths of the cast INCONEL 718 critical grade alloy at the analysis temperature of 210 °R. These two values were obtained from Ref. 2, in which average yield and ultimate strengths were determined from three specimen tests at 210 °R. The values presented at 210 °R are predicted minimum values for the critical grade casting with heat treatment according to STA-1. Yield strength was determined to be 125.1 ksi (average predicted minimum). Ultimate strength was determined to be 149.4 ksi (average predicted minimum).

Specification of Young's Modulus and Poisson's Ratio versus temperature for use by ANSYS was obtained wholly from the Rocketdyne Materials Properties Manual. The property data were curve fitted to cubic polynomials for use by ANSYS over the temperature range of 0 to 2000 °R. Young's Modulus and Poisson's Ratio for INCONEL 718 as functions of absolute temperature are presented in Figures 15 and 16, respectively.

5. STRUCTURAL ANALYSIS/RESULTS

The ANSYS HPOTP preburner pump housing finite element model was used to determine the static stress distribution for SSME engine operation at FPL with only axial misalignment limit loads applied to the inlet and discharge flange. Margins of safety were not computed because the maximum load conditions were not analyzed due to the absence of torque, moments, and shear acting on the inlet and discharge pipe flange. These loads would naturally arise from moderate to maximum allowable misalignment.

Stress plots of the vane elements viewed from the inlet side of the pump housing are shown in Figures 17 through 22. Even with almost symmetric loading, the vanes exhibit an asymmetric stress state due to the asymmetric housing geometry. Comparisons of Figures 17 and 18 and Figures 20 and 21 reveal that the axial (Sigma-Z) stress is the major contributor to the maximum principal stress (Sigma-1). Table 8 lists the first four ANSYS calculated maximum Von Mises nodal stresses (Sigma-E) in the housing, their nodal locations, and corresponding factors of safety based on yield strength. Table 9 presents the highest four maximum principal stresses and their nodal locations.

It must be emphasized that the stresses and factors of safety presented in Tables 8 and 9 do not represent the worst load case. The worst load case will include all allowable misalignment loads (torque, moments, shear, and axial), along with vane stresses that will be the product of both applied oxidizer pressures and support bolt loads.

Examination of Table 9 shows that all four highest maximum principal stresses occur at the corner made by a vane element with the inlet side of the housing. Fillets were not modeled in this region because that degree of refinement would almost certainly have necessitated substructuring. It is of greater advantage to have an unsubstructured model in the event of loads that

produce plastic stress regions for future load cases. A further obstacle to model refinement would be exceeding the ANSYS wavefront limit, which condition was rapidly approached during model development.

Figures 23 through 27 show various stress components of several housing cross sections. Comparison of Figures 25 and 26 again reveals that the axial stress is the major contributor to the maximum principal stress in the region of the vanes.

Considering the result that the vane region is the area of highest stress, the question is whether the applied loads in the proximity of each diffuser vane are realistic. Certainly, the pressure differential between the pressure and suction sides of each vane, which is presently not known, has an unknown general effect on the stresses in this critical region. Additionally, circumferential pressure variation in the housing (it should be possible to estimate this based on the geometry and fluid) will have an overall effect on all the vane stresses. Support bolt loads will add to the high axial stresses in localized vane regions.

6. SUMMARY

Maximum stresses at each cross section almost always occurred on the suction side of each vane at the vane's intersection with the inlet side of the housing. The principal contributor to these stresses was the axial stress which developed as a result of the passage pressures acting on the volute geometry.

The stiffening webs served to reduce these stresses locally, but stresses were maximized not only at the vane-housing intersection but also at each vane nose and tail. The corner made by the vane suction side, vane nose (or tail) end, and the housing inlet side was typically an area of highest stress.

Examination of the stress contours of various housing cross sections shows a well defined region at which maximum passage stresses occur. Passage stresses range from a low of about 4 ksi to a maximum of from 40 to 50 ksi. Minimum passage stresses occur in regions where the pressure surface is convex and maximum generally where the pressure surface is concave and has the smallest radius of curvature.

Overall cross-section stresses fall as the passage grows in size. Discharge pipe stresses are small. The principal stress in the discharge pipe ranges from approximately 11 to 40 ksi.

Although the results for the load case presented here indicate ample factors of safety, further investigation is required. If a realistic three-dimensional (3-D) stress state within the housing is sought, then it is not enough to have a 3-D finite element model. The load variation in three dimensions must be known as well. Knowledge of passage pressures versus station angle, pressure differentials across each vane, and support bolt loads must be included to obtain the true worst case stress state and, ultimately, to improve the design.

7. RECOMMENDATIONS

In order to perform a complete structural analysis of the HPOTP preburner pump housing, the following would be required.

1. A static analysis should be performed which includes specified limit load moments, torques, and shear forces on both the discharge pipe flange and the pump housing inlet. The analysis of this case would provide the maximum allowable load case for the steady-state engine operation at FPL.
2. Detailed knowledge of fluid pressure within the housing, including pressure variation with station angle and within each cross section. Of special importance is the pressure drop across the vanes. This pressure drop causes shear on the vanes and adds to the overall vane stress state.
3. Pressure fluctuation magnitudes would serve to provide the means for obtaining realistic high and low cycle fatigue life estimates when used in conjunction with this ANSYS model. Knowledge of stress amplitudes and maximum stresses provides the operating stress ratio for determination of both low and high cycle fatigue life.
4. It is recommended that a modal analysis be performed using this model to determine possible resonant conditions with pressure fluctuation and impeller wake frequencies. Reference 3 also recommended this work. The 3-D pump housing model is ideally suited to providing modal frequencies for a dynamic analysis.
5. Investigation of porosity leakage cannot be performed using two-dimensional models or the 3-D model presented here. Two-dimensional models cannot allow for asymmetric misalignment loads or pressure variation with station angle. The 3-D model presented here is too large and complex to include support bolt hole geometry and the details of vane nose and tail geometry. The qualities lacking in the above mentioned models are important in considering the leakage, since it has been found to occur in the region between support bolt holes and vanes. It is recommended that about half of the full 3-D model be refined and detailed as a separate model to investigate stresses in the support bolt hole-to-vane region. This would allow for application of some asymmetric misalignment loads, while still providing for detailed modeling in the region where the leakage has been discovered.

6. Reference 2 provides low cycle fatigue life data for the preburner pump housing material; however, these data were obtained while testing at a stress ratio of $R=-1.0$. This is an unrealistic number for examination of the low or high cycle fatigue life characteristics of the preburner pump housing. In addition, the heat treatment of the specimens tested was in accordance with RA0611-020, whereas the heat treatment specification for the preburner pump housing material is RB0170-155. Reference 4 also presents a plot of low cycle fatigue life in the form of a plot of strain amplitude versus reversals to failure, but the stress ratio at which these tests were performed is not given. Cyclic stress-strain data should be produced or experimentally determined for the housing material at a stress ratio of zero or greater than zero to avoid underprediction of housing life. This is the type of fatigue environment to which the housing is subjected during SSME engine operation.

Once the above information is obtained, the following results could be achieved:

1. Prediction of low and high cycle fatigue life for the preburner pump housing
2. Prediction of maximum steady state and transient stress levels within the housing
3. Prediction of minimum margins of safety for the preburner pump housing
4. Judgment of whether the design geometry contributes significantly to the possibility of oxidizer leakage into support bolt holes
5. Resonant conditions during engine operation in the preburner pump housing.

8. REFERENCES

1. Drawing RS007739, HPOTP Preburner Pump Housing.
2. Internal Letter from D.M. Haegelin to R.M. Passerini, Report No. MPR-87-1029 (23071), Cyclic Stress-Strain Diagram for INCONEL 718, Cast, STA-1, Rockwell International, November 11, 1987.
3. Structural Audit, Action Item OX157.
4. Internal Letter from A.P. Meisels to (Unknown), Report No. MPR-87-0407 (13701), Structural Audit-Materials, Preburner Pump Volute HPOTP, INCONEL 718C, Rockwell International, May 4, 1987.

Table 1 ELEMENT MATERIAL AND TYPE NUMBERS FOR GLOBAL ELEMENT REGIONS

MODEL REGION	TYPE NUMBER	MATERIAL NUMBER	NUMBER OF ELEMENTS
Diffuser Vanes	4	4	79
Webs Stiffening the Passage	4	3	520
Symmetric Inlet Region	5	2	2740
Preburner to Main Pump Housing Flange	8	1	240
General Elements	1	1 and 2	8712

Table 2 ELEMENT MATERIAL AND TYPE NUMBERS FOR ELEMENTS NOT IN THE TONGUE REGION

MODEL REGION	TYPE NUMBER	MATERIAL NUMBER	NUMBER OF ELEMENTS
Elements Adjacent to Vanes to which Pressures are Applied	4	2	582
Square Bolts Modeling Shroud Seal and Shroud Ring Bolts	6	3	20
Wedge elements in the Passage Region	2	1	714
Inner Radius Elements of the Passage	3	1	663

Table 3 ELEMENT MATERIAL AND TYPE NUMBERS FOR ELEMENTS IN THE TONGUE REGION

MODEL REGION	TYPE NUMBER	MATERIAL NUMBER	NUMBER OF ELEMENTS
Element Region on the Inlet Side of the Vanes	12	2	550
Pressure Surface Adjacent to Vanes on Inlet Side of Housing	12	4	30
Inner Radius Elements of the Passage	13	1	225
Tongue	14 and 15	1	134
Beginning of the Discharge Pipe near the Passage	16	1	280
End of the Discharge Pipe including the Flange	17	2	205

Table 4 NODE ANGLE LOCATIONS FOR NODES FROM -25° TO 147°,
EXCEPT ON DISCHARGE PIPE

Model Station Number	Nodes on Main Pump Side of Vanes and Nodes on the Preburner to Main Pump Housing Flange	Passage Region and Symmetric Inlet Region
1	-25	-27
2	-21	-21
3	-15	-15
4	-10 b.c.	-9
5	-5	-3
6	5	3
7	10 b.c.	9
8	15	15
9	21	21
10	25	27
11	30 b.c.	33
12	35	39
13	45	45
14	50 b.c.	51
15	55	57
16	65	63
17	70 b.c.	69
18	75	75
19	85	81
20	90 b.c.	87
21	95	93
22	99	99
23	105	105
24	110 b.c.	111
25	115	117
26	125	123
27	130 b.c.	129
28	135	135
29	141	141
30	145	147

Table 5 NODE ANGLE LOCATIONS FOR NODES FROM 150° TO -30°,
EXCEPT ON DISCHARGE PIPE

Station Number	Nodes on Main Pump side of vanes and nodes on the Preburner to Main Pump Housing Flange	Passage Region and Symmetric Inlet Region
31	150 b.c.	153
32	155	159
33	165	165
34	170 b.c.	171
35	175	177
36	-175	-177
37	-170 b.c.	-171
38	-165	-165
39	-155	-159
40	-150 b.c.	-153
41	-145	-147
42	-141	-141
43	-135	-135
44	-130 b.c.	-129
45	-125	-123
46	-115	-117
47	-110 b.c.	-111
48	-105	-105
49	-95	-99
50	-90 b.c.	-93
51	-85	-87
52	-81	-81
53	-75	-75
54	-70 b.c.	-69
55	-65	-63
56	-55	-57
57	-50 b.c.	-51
58	-45	-45
59	-35	-39
60	-30 b.c.	-33

Table 6 NUMBERING SCHEME FOR NODES FROM -21° TO 147° ,
EXCEPT FOR WEB AND FLANGE NODES

Model Station Number	Starting Node Number	Final Node Number
2	304	606
3	607	909
4	910	1212
5	1213	1515
6	1516	1818
7	1819	2121
8	2122	2424
9	2425	2727
10	2728	3030
11	3031	3333
12	3334	3636
13	3637	3939
14	3940	4242
15	4243	4545
16	4546	4848
17	4849	5151
18	5152	5454
19	5455	5757
20	5758	6060
21	5759	6363
22	6364	6666
23	6667	6969
24	6970	7272
25	7273	7575
26	7576	7878
27	7879	8181
28	8182	8484
29	8485	8787
30	8788	9090

Table 7 NUMBERING SCHEME FOR NODES FROM 150° TO -75°,
EXCEPT FOR WEB AND FLANGE NODES

Model Station Number	Starting Node Number	Final Node Number
31	9091	9393
32	9394	9696
33	9697	9999
34	10000	10302
35	10303	10605
36	10606	10908
37	10909	11211
38	11212	11514
39	11515	11817
40	11818	12120
41	12121	12423
42	12424	12726
43	12727	13029
44	13030	13332
45	13333	13635
46	13636	13938
47	13939	14241
48	14242	14544
49	14545	14847
50	14848	15150
51	15151	15453
52	15454	15756
53	15757	16059

Table 8 MAXIMUM HOUSING VON MISES STRESSES

NODE	REGION	VON MISES STRESS (ksi)	FACTOR OF SAFETY ON YIELD
5857	On inlet side of vane region at $\theta = 87^\circ$	67.0	1.87
4341	On inlet side of housing near a vane corner at $\theta = 57^\circ$	66.2	1.89
4342	On inlet side of vane region at $\theta = 57^\circ$	65.7	1.90
1009	On inlet side of vane region at $\theta = -9^\circ$	65.7	1.90

Table 9 MAXIMUM HOUSING PRINCIPAL STRESSES

NODE	REGION	PRINCIPAL STRESS (ksi)
1008	On inlet side of housing at a vane corner at $\theta = -9^\circ$	84.7
4341	On inlet side of housing at a vane corner at $\theta = 57^\circ$	80.6
7674	On inlet side of housing at a vane corner at $\theta = 123^\circ$	78.1
4633	On inlet side of housing at a vane corner at $\theta = 63^\circ$	77.6

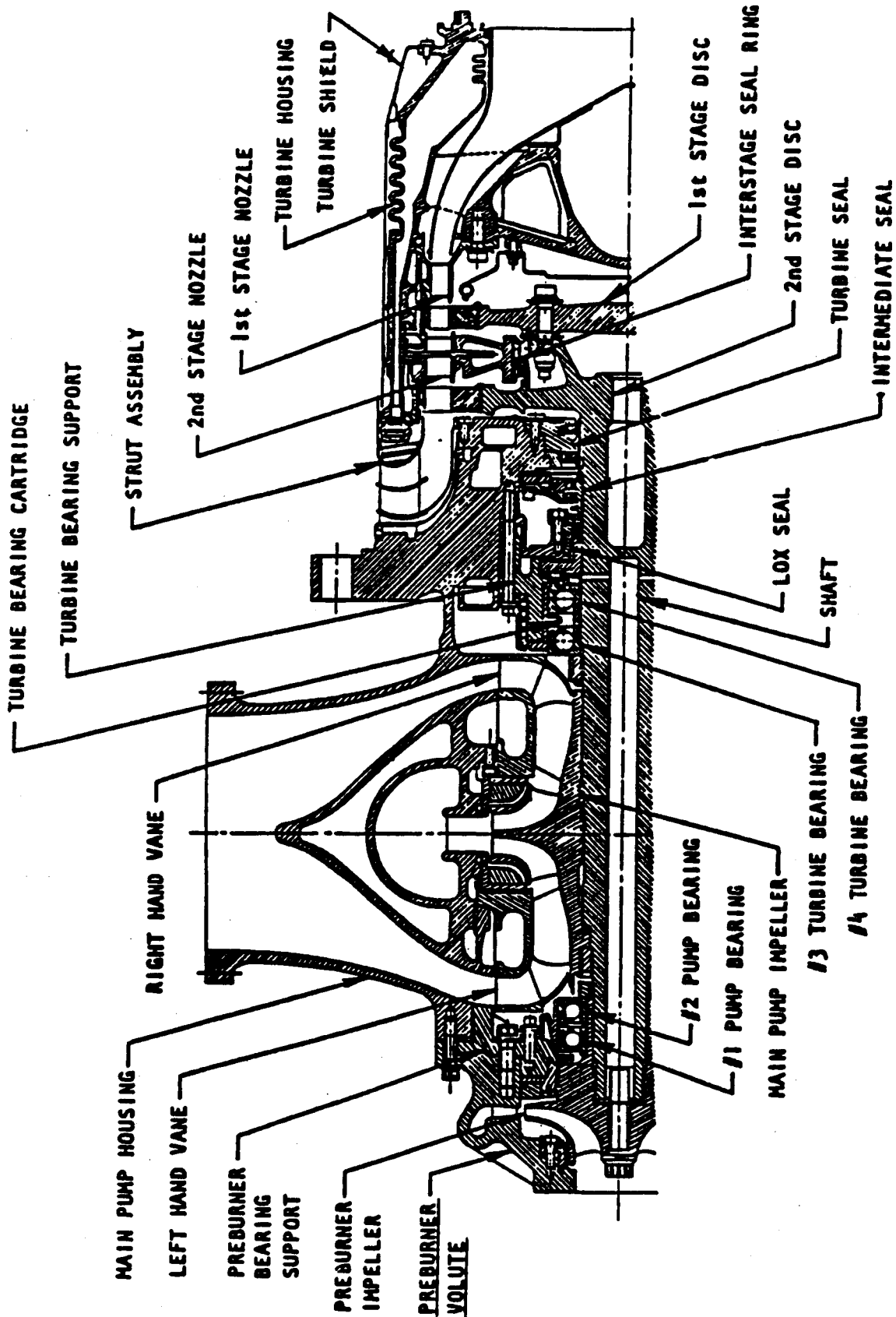


Figure 1 Schematic of the HPOTP Major Components

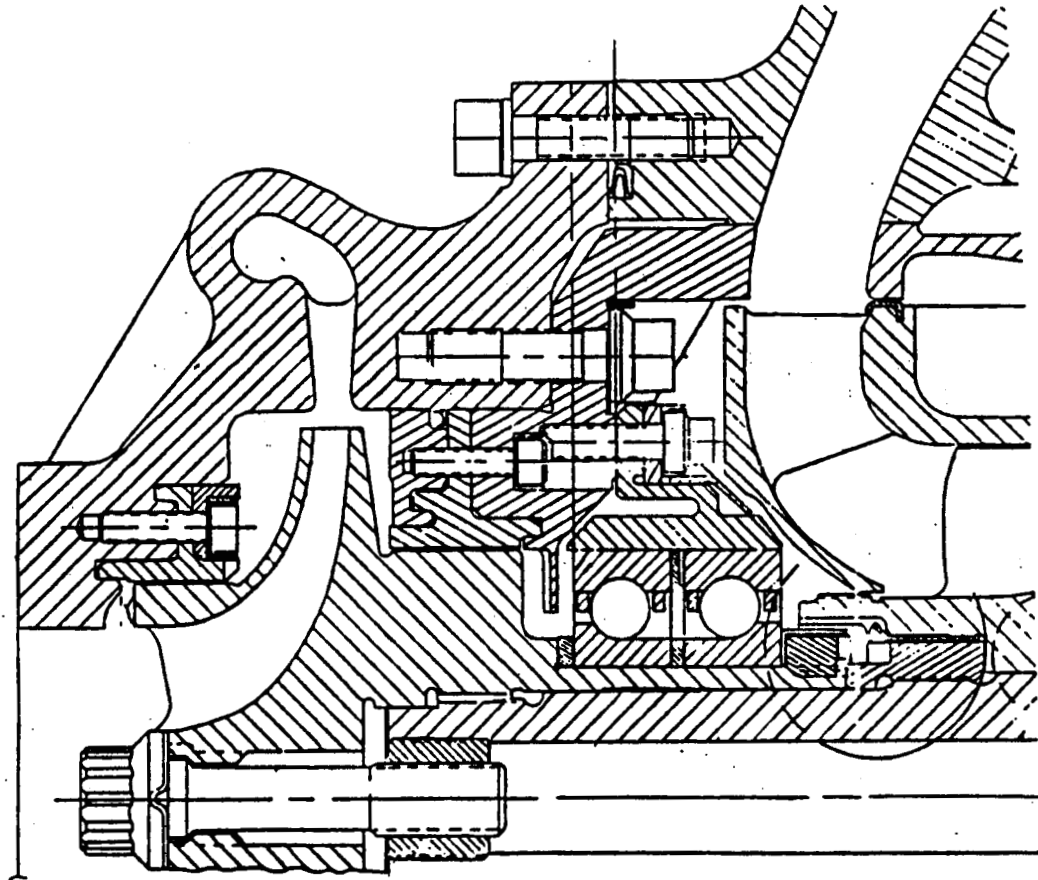


Figure 2 Preburner Pump Housing and Preburner Pump Components

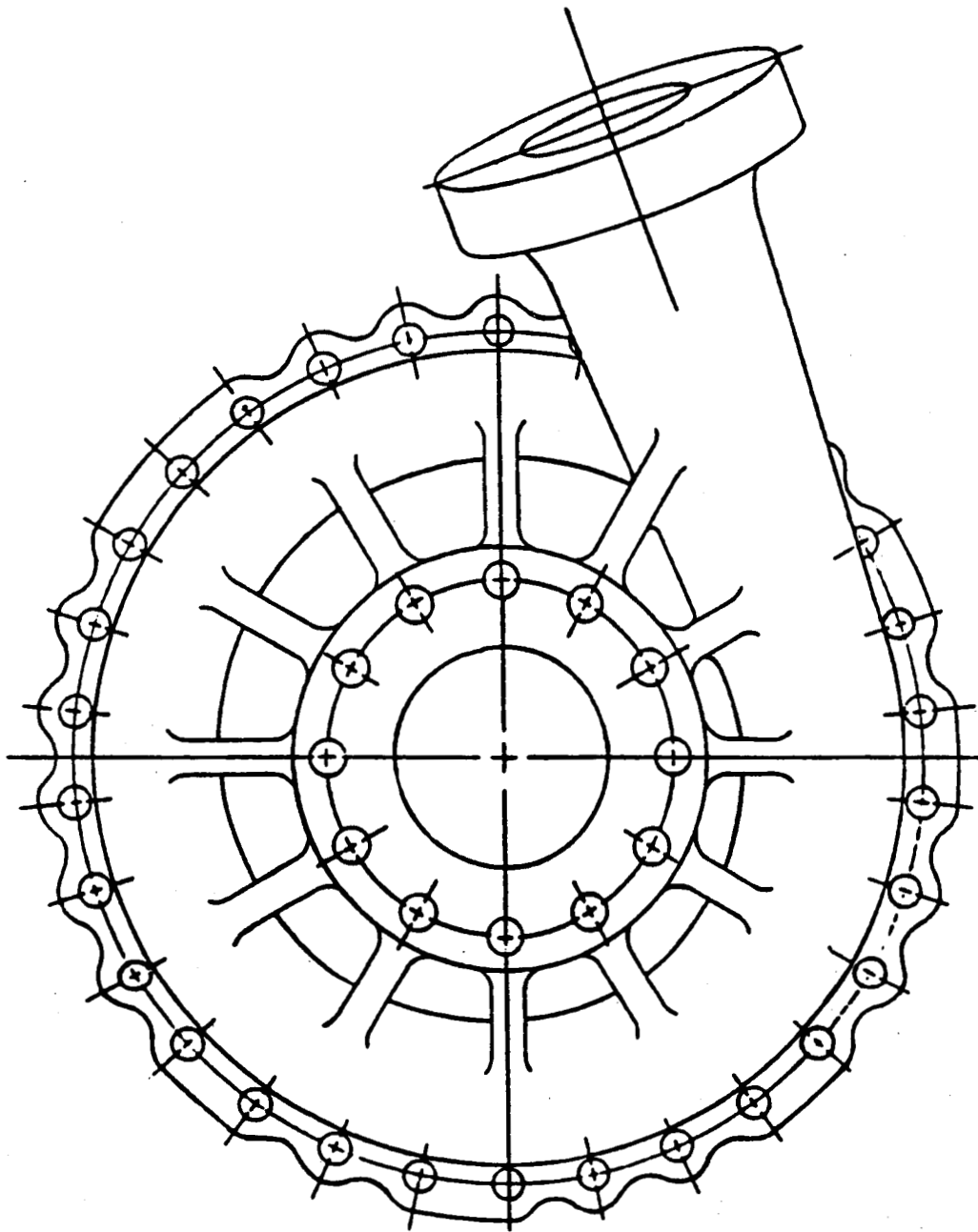


Figure 3 Preburner Pump Housing View from Inlet Side

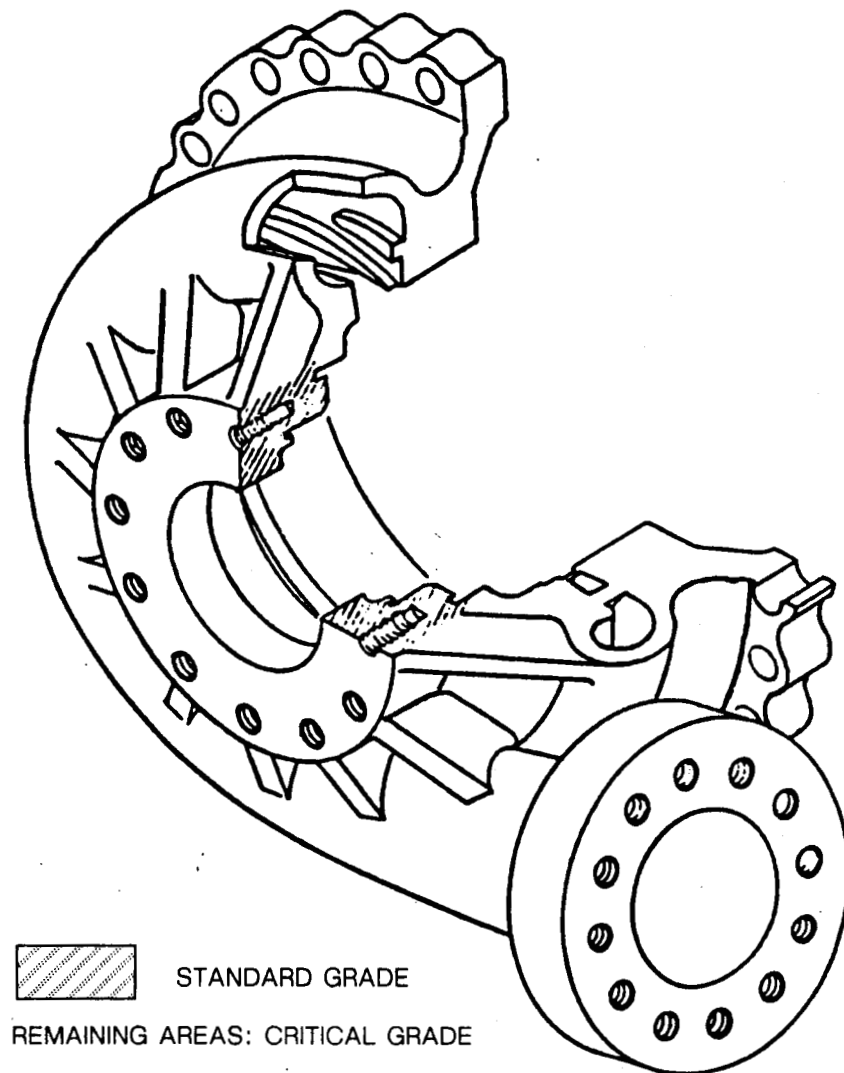


Figure 4 Cutaway View of Preburner Pump Housing

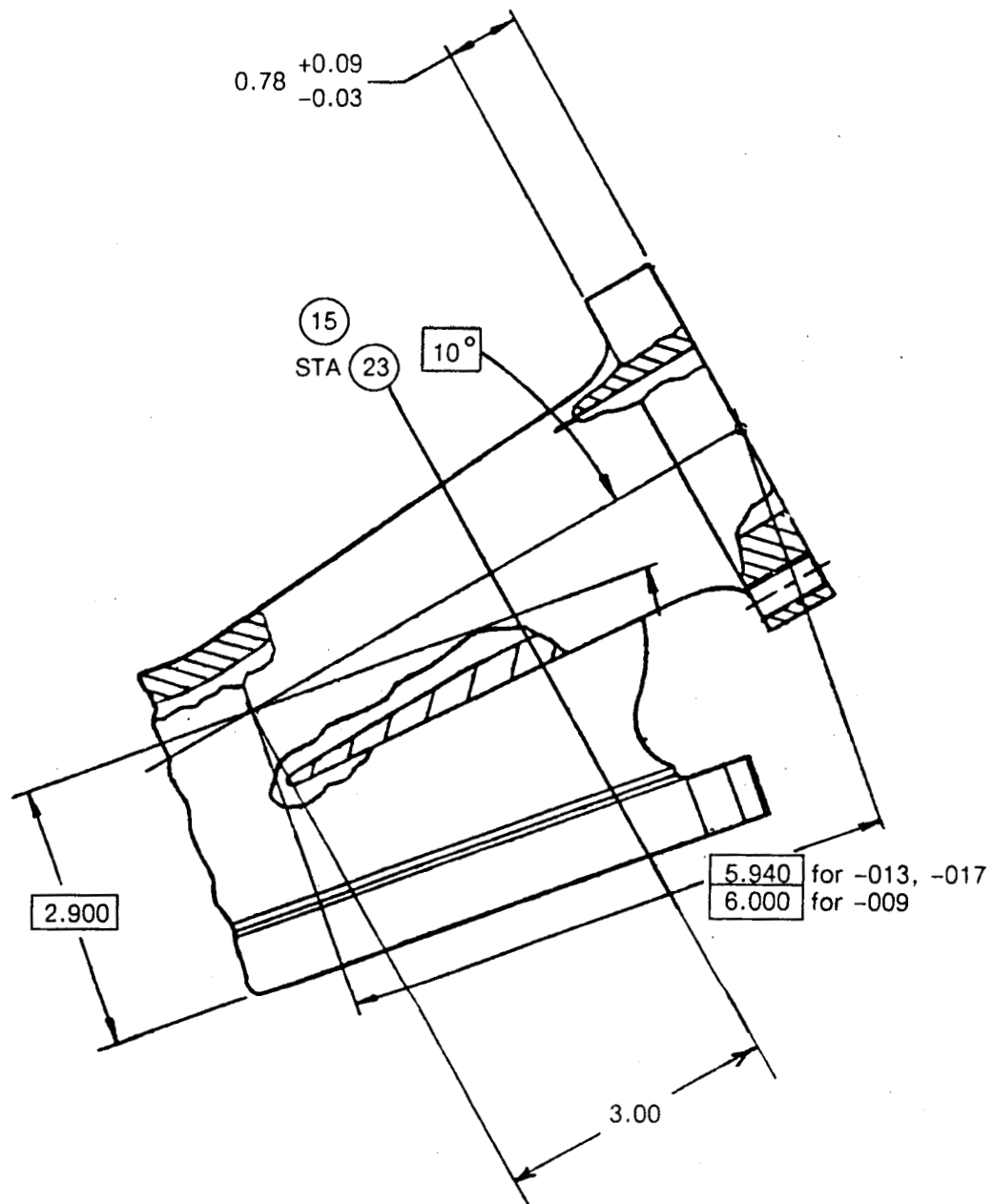


Figure 5 Orientation of Discharge Pipe with respect to Pump Housing Volute Passage

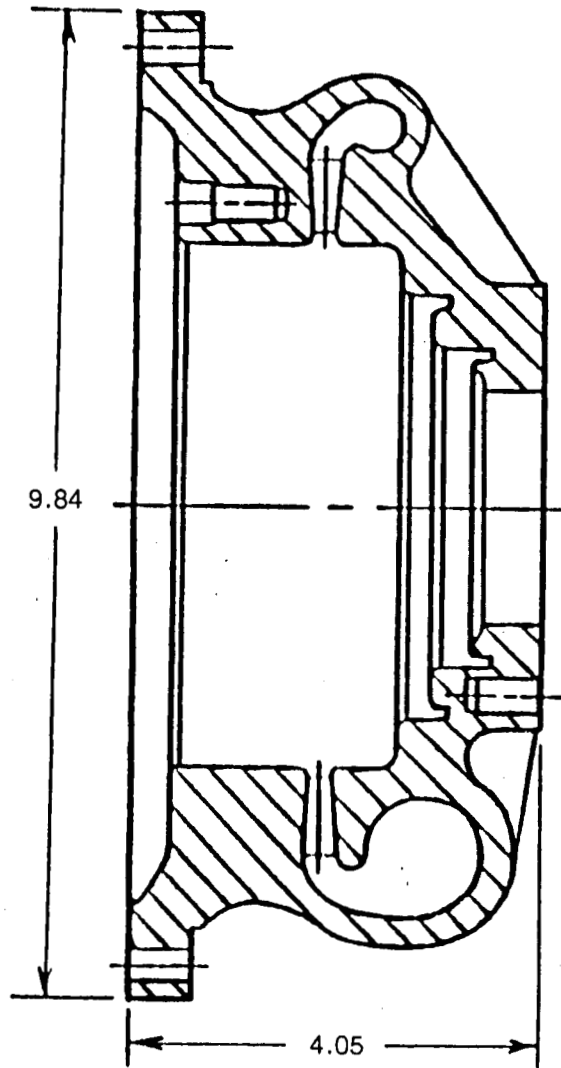


Figure 6 Overall Dimensions of the Preburner Pump Housing

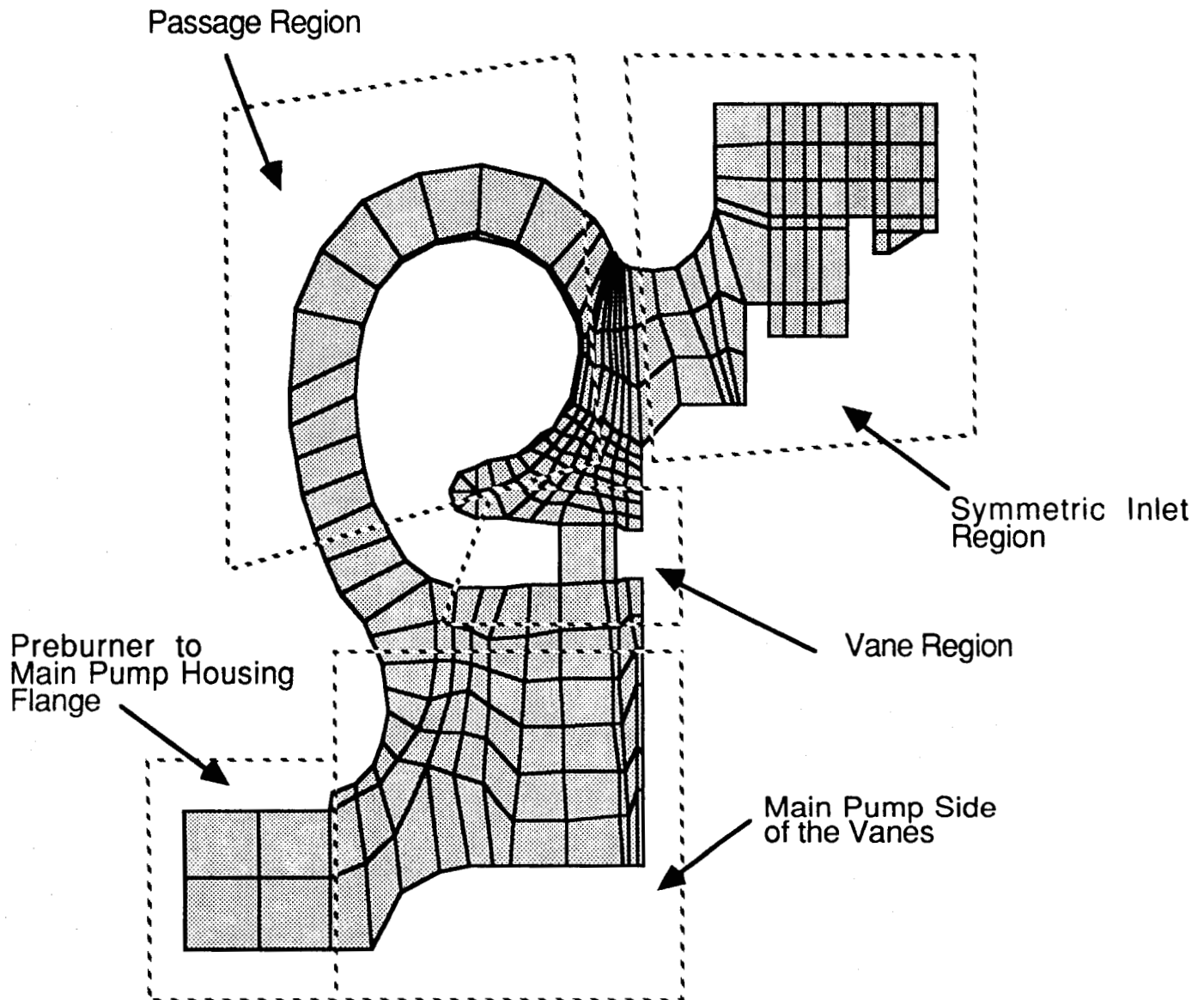


Figure 7 Cross-Section Regions of the Model

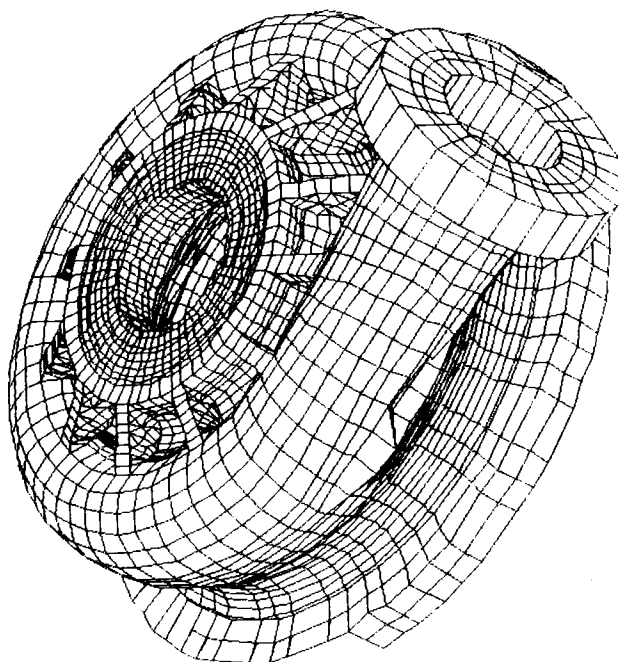


Figure 8 Preburner Pump Housing Model Plot, View A from Inlet Side

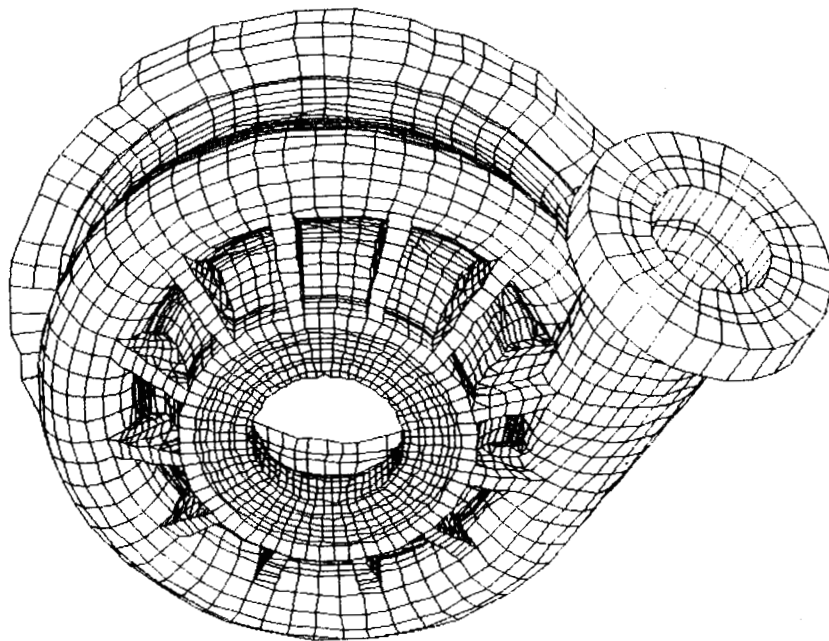


Figure 9 Preburner Pump Housing Model Plot, View B from Inlet Side

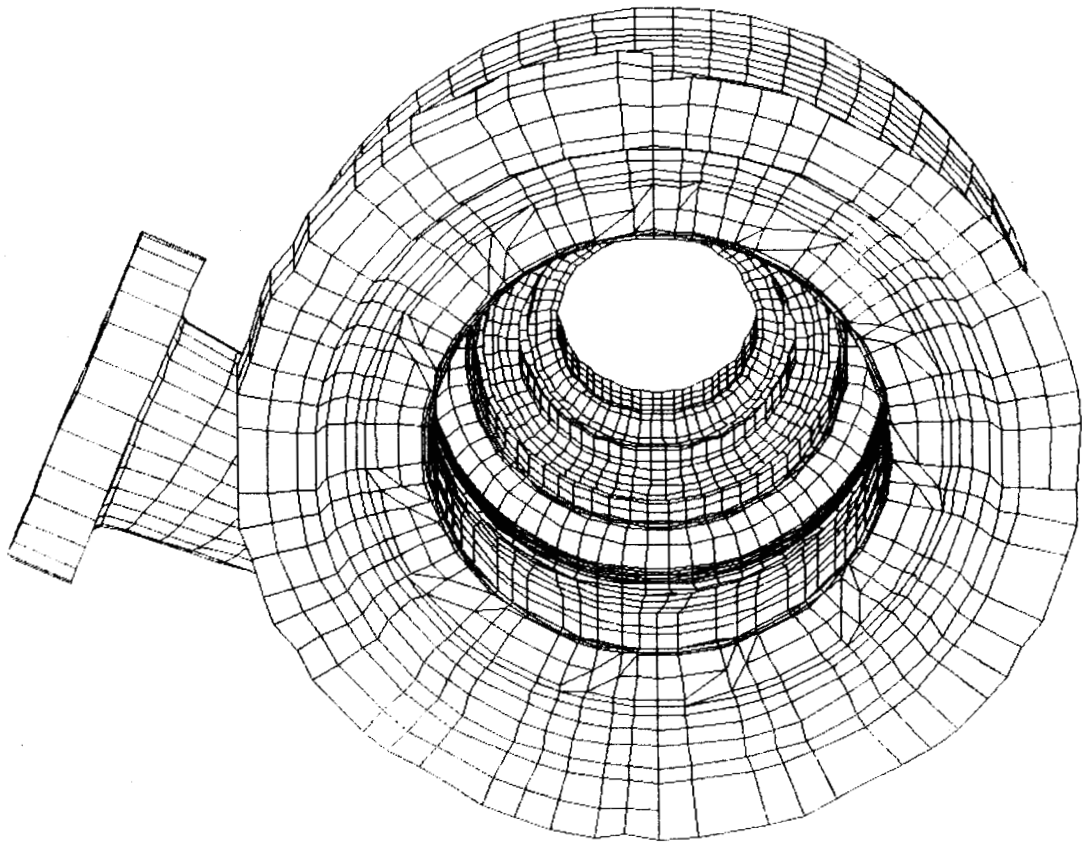


Figure 10 Preburner Pump Housing Model, View from Main Pump Side

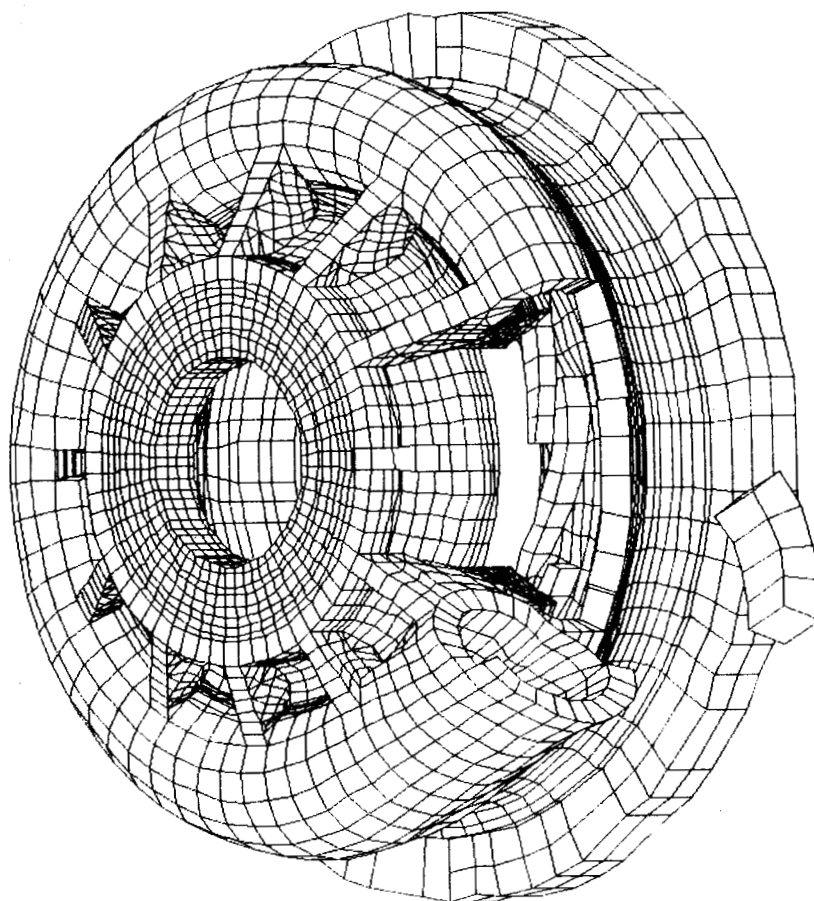


Figure 11 Cutaway View of Preburner Pump Housing Model

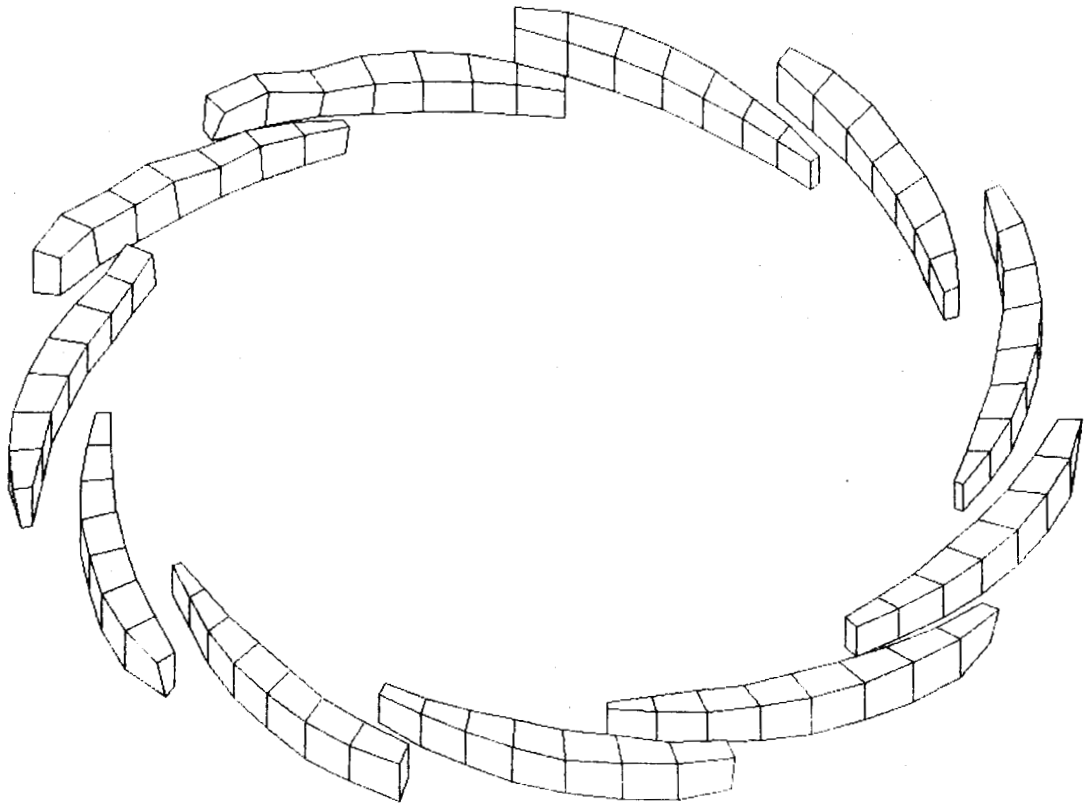


Figure 12 Diffuser Vane Elements

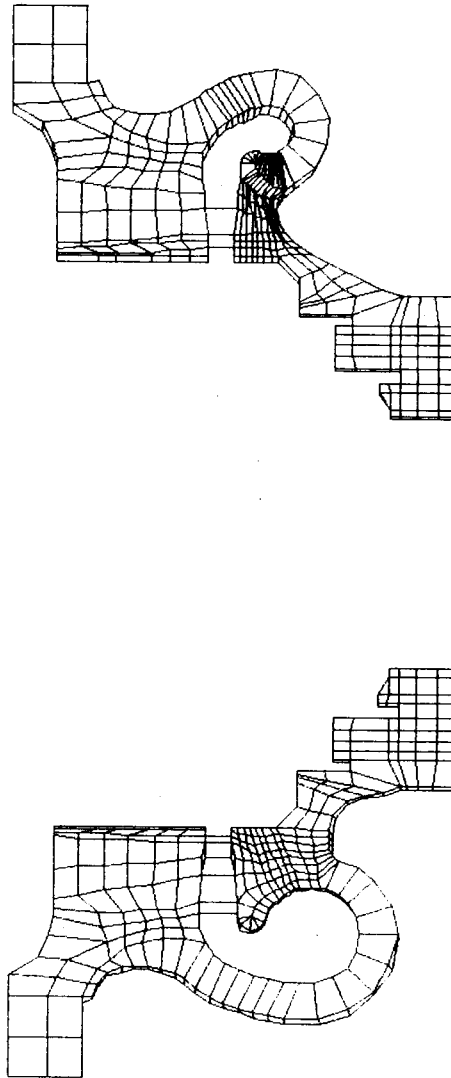
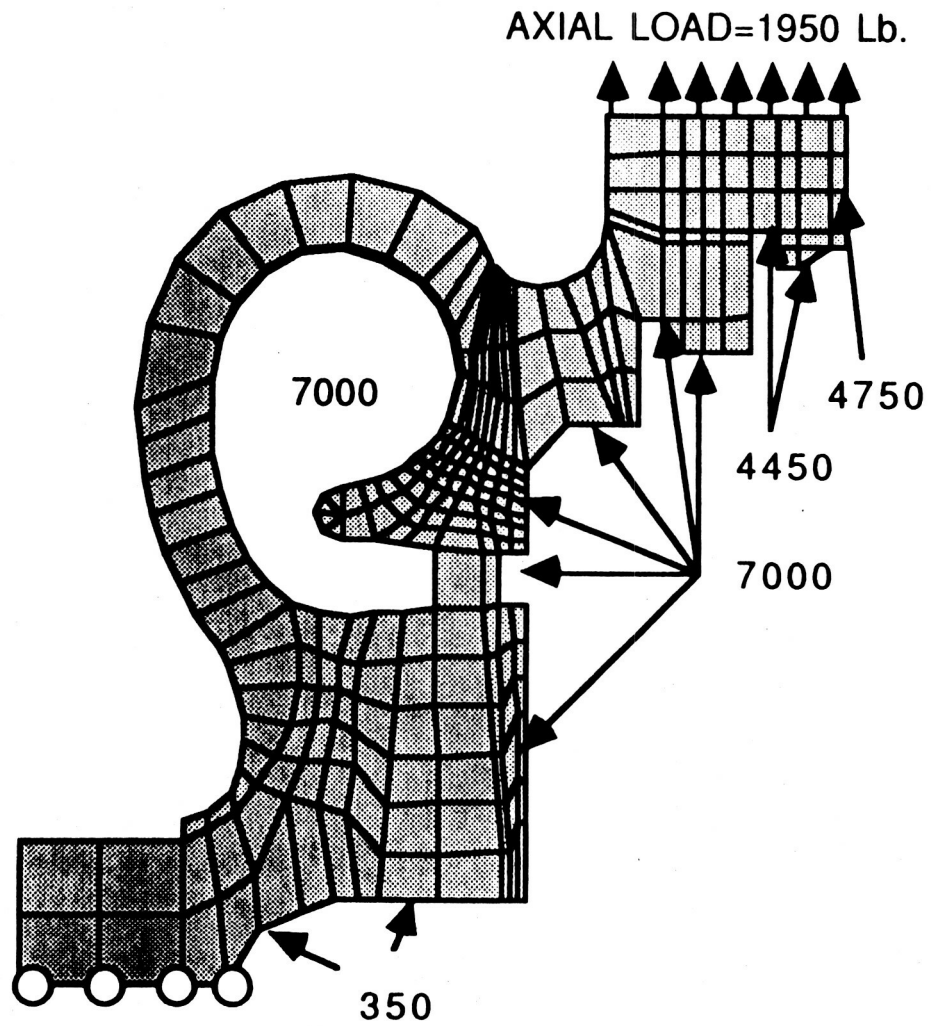


Figure 13 Two Preburner Pump Model Cross Sections 180° Apart



Circled Nodes completely constrained
around entire circumference

Figure 14 Pressure Loads and Boundary Conditions

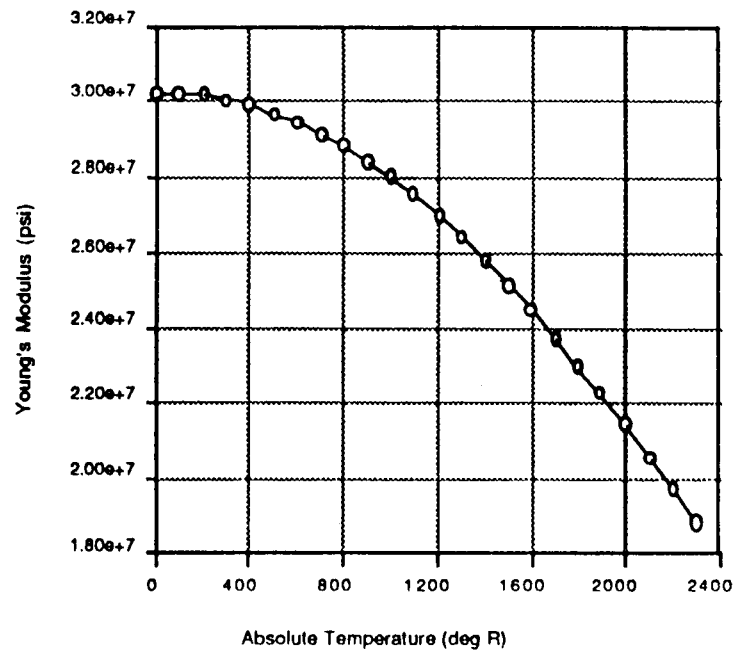


Figure 15 INCONEL 718 Young's Modulus as a Function of Absolute Temperature (Rankine)

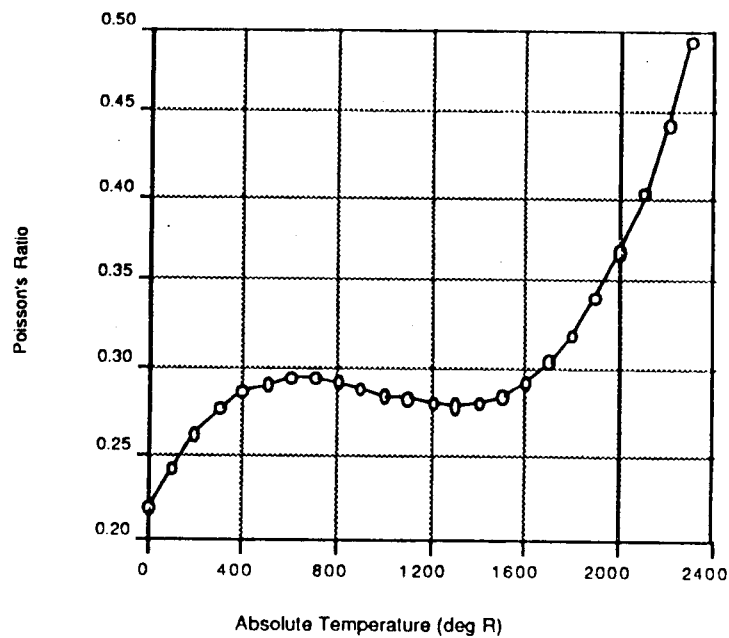


Figure 16 INCONEL 718 Poisson's Ratio as a Function of Absolute Temperature (Rankine)

ANSYS 4.3
APR 4 1989
10:50:11
POST1 STRESS
STEP=1
ITER=1
SIG1 (AVG)

ZV=1
DIST=3.72
XF=-.037
YF=-.0628
ZF=1.95
HIDDEN
MX=88266
MN=27886
34594
41303
48012
54721
61430
68139
74848
81557
88266

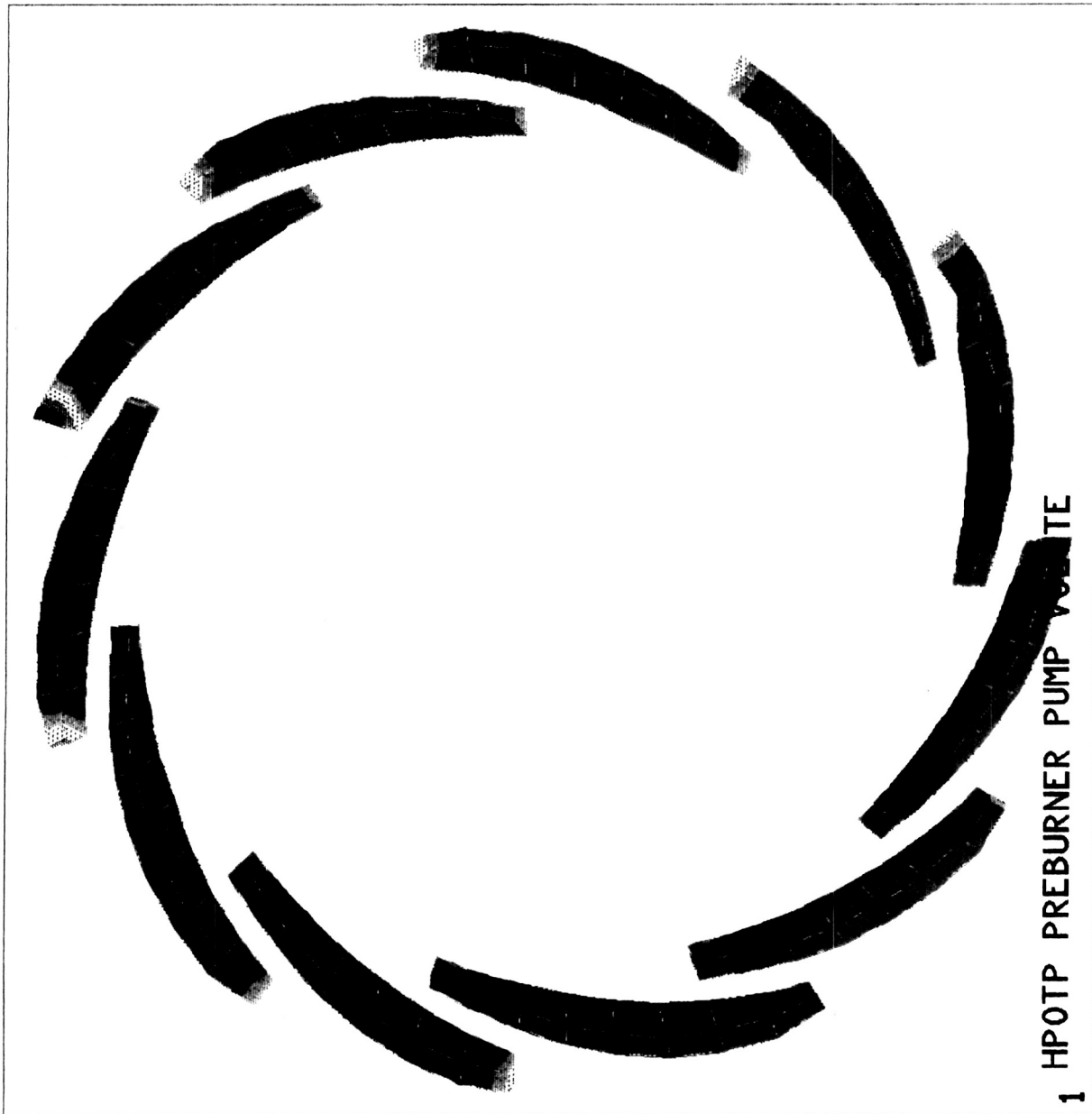


Figure 17 Vanes Viewed from Inlet Side, Sigma -1 (Maximum Principal Stress)

ORIGINAL PAGE
COLOR PHOTOGRAPH

ANSYS 4.3
 APR 4 1989
 11:03:00
 POST1 STRESS
 STEP=1
 ITER=1
 SZ (AVG)
 CSYS=1
 ZV=1
 DIST=3.72
 XF=-.037
 YF=-.0628
 ZF=1.95
 HIDDEN
 MX=77400
 MN=18367
 24923
 31483
 38043
 44603
 51163
 57723
 64283
 70843
 77400

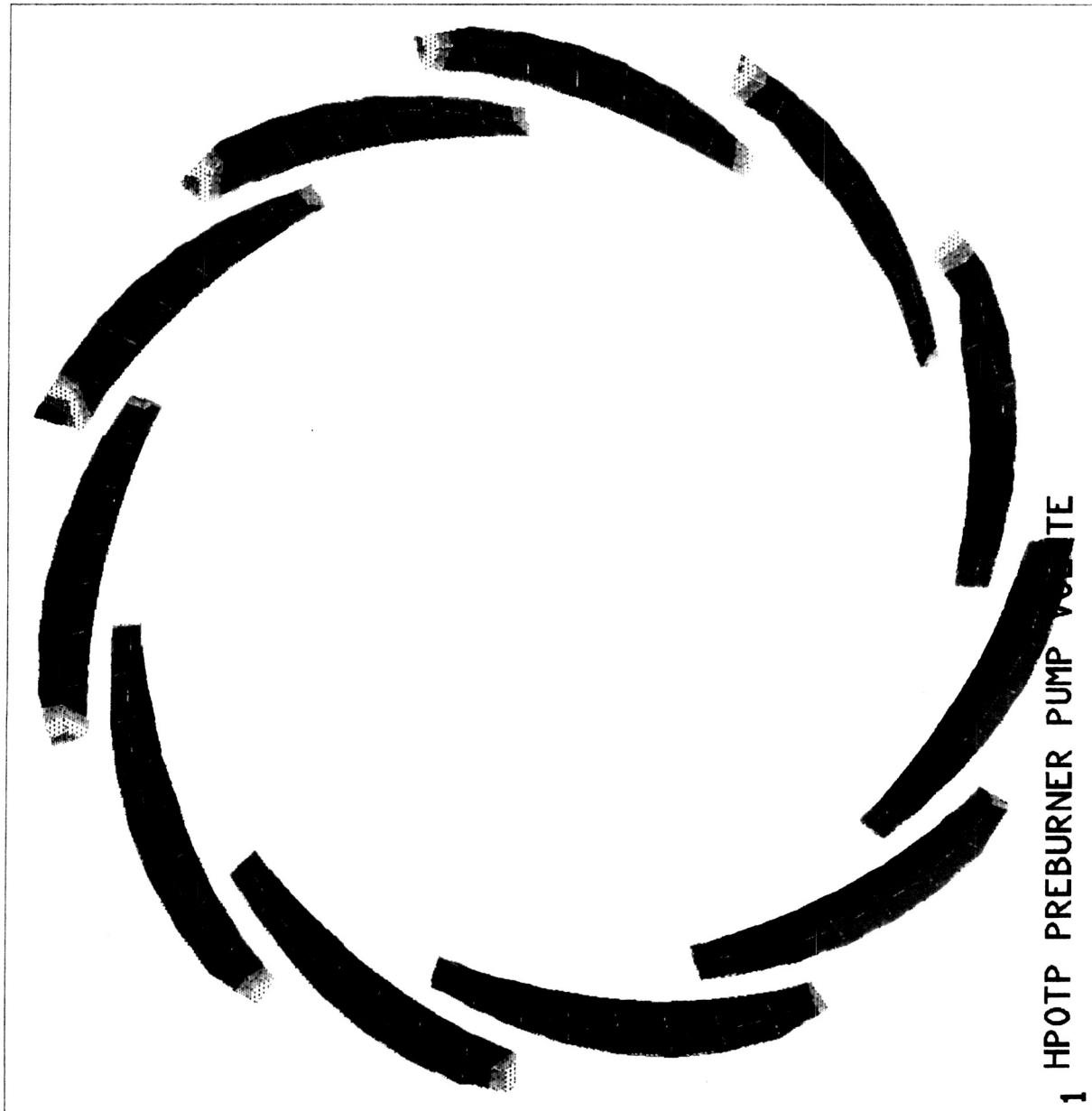


Figure 18 Vanes Viewed from Inlet Side, Sigma -Z (Axial Stress)

ORIGINAL PAGE
 COLOR PHOTOGRAPH

ORIGINAL PAGE
COLOR PHOTOGRAPH

ANSYS 4.3
APR 4 1989
11:27:36
POST1 STRESS
STEP=1
ITER=1
SIGE (AVG)

ZV=1
DIST=3.72
XF=-.037
YF=-.0628
ZF=1.95
HIDDEN
MX=80989
MN=31758
37225
42696
48167
53638
59109
64580
70051
75522
80989

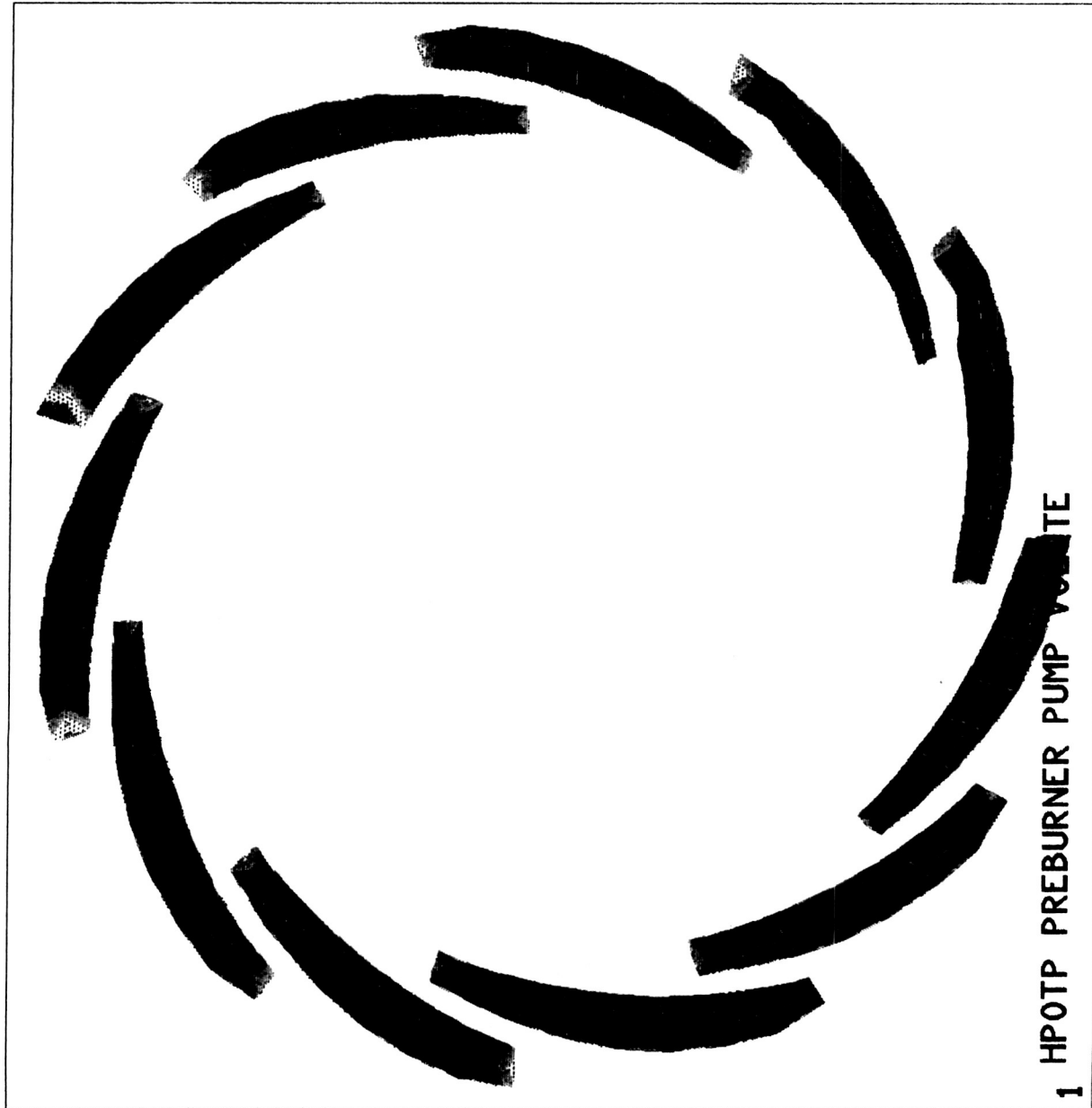


Figure 19 Vanes Viewed from Inlet Side, Sigma -E
(Von Mises Equivalent Stress)

ANSYS 4.3
APR 4 1989
14:24:50
POST1 STRESS
STEP=1
ITER=1
SIG1 (AVG)

ORIGINAL PAGE
COLOR PHOTOGRAPH

ZV=-1
DIST=3.72
XF=-.037
YF=-.0628
ZF=1.95
MX=88266
MN=27886
34594
41303
48012
54721
61430
68139
74848
81557
88266

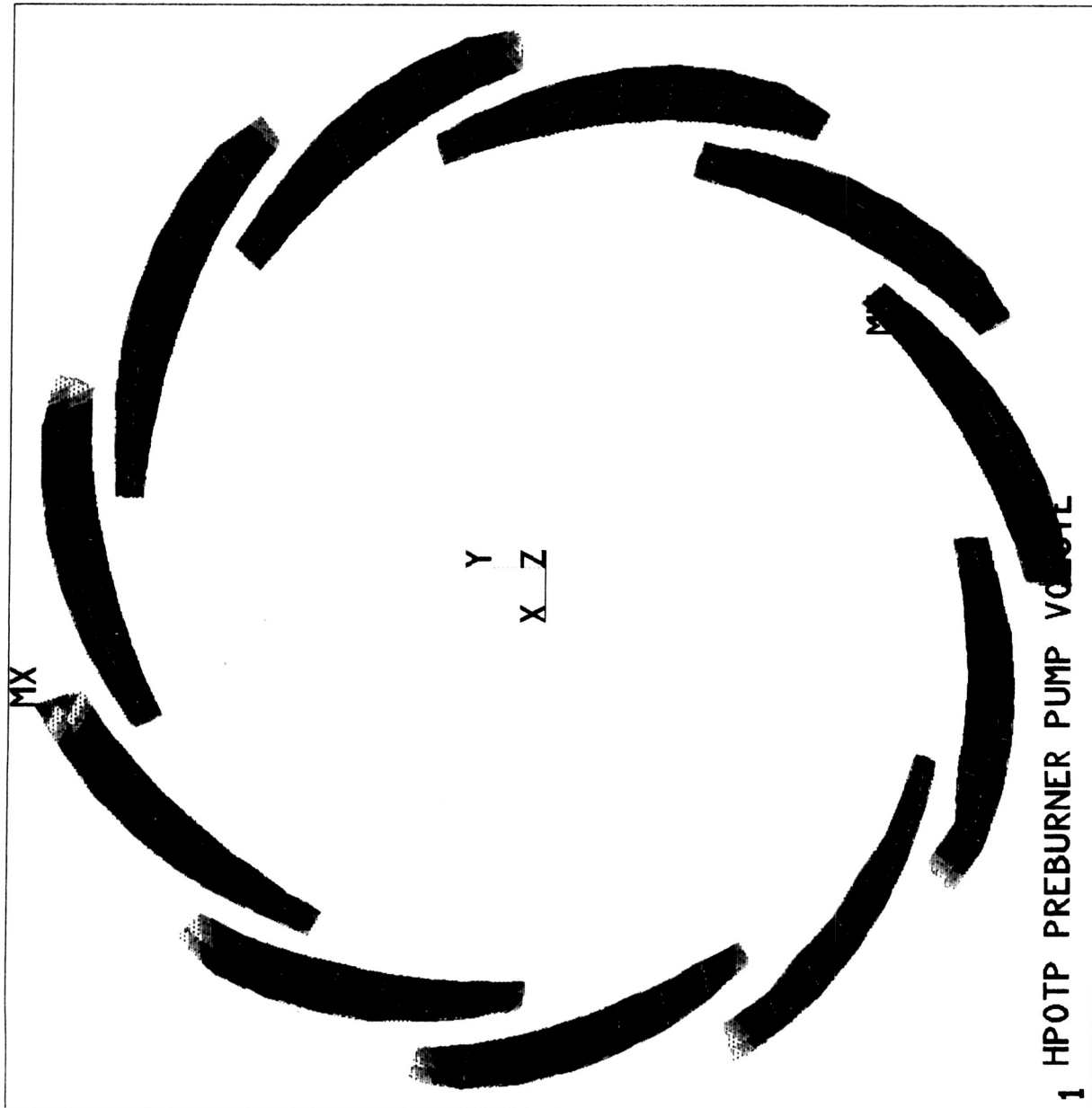


Figure 20 Vanes Viewed from Pump Side, Sigma -1

ORIGINAL PAGE
COLOR PHOTOGRAPH

ANSYS 4.3
APR 4 1989
14:42:39
POST1 STRESS
STEP=1
ITER=1
SZ (AVG)
CSYS=1

ZV=-1
DIST=3.72
XF=-.037
YF=-.0628
ZF=1.95
MX=77400
MN=18367
24923
31483
38043
44603
51163
57723
64283
70843
77400

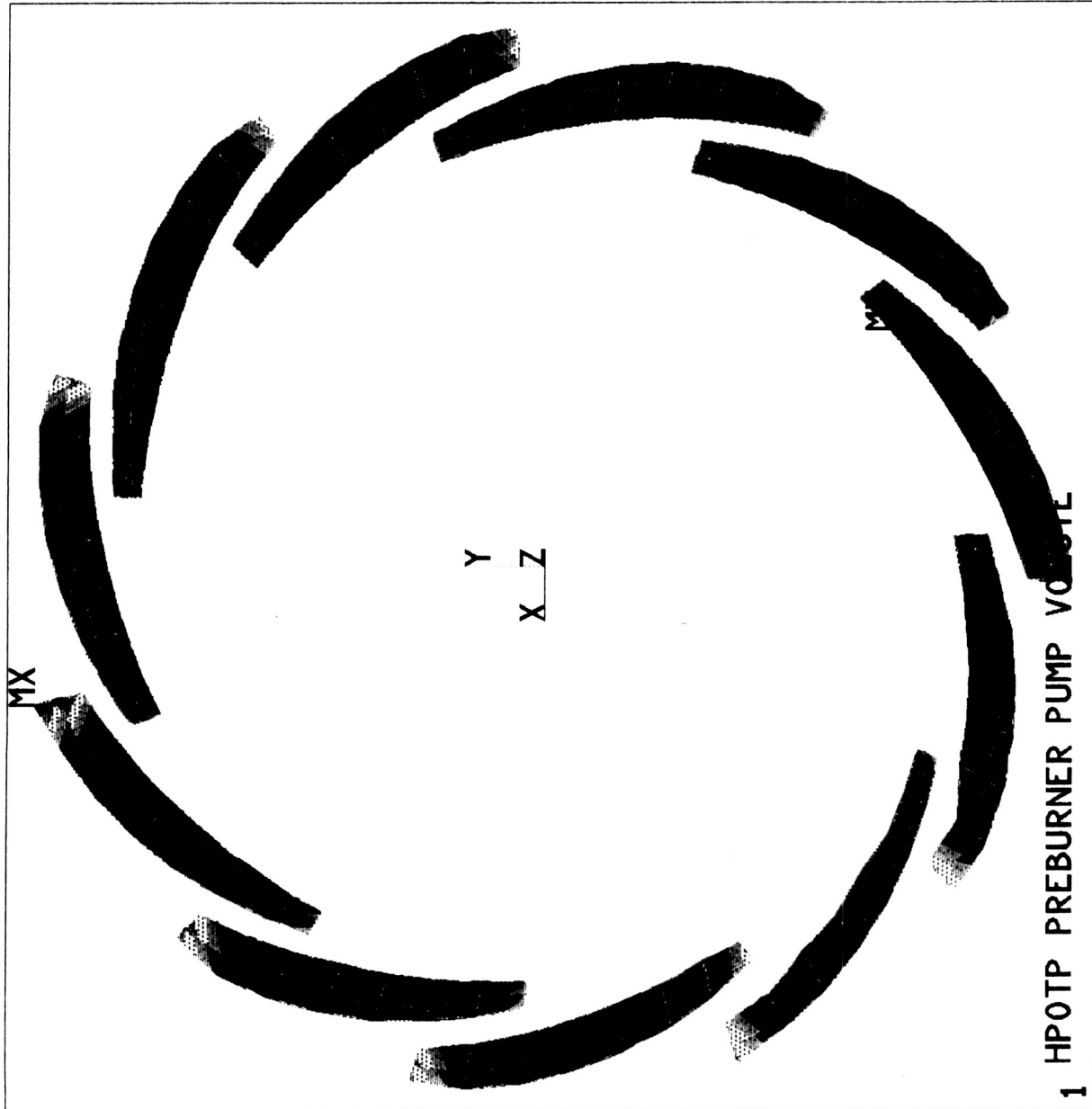


Figure 21 Vanes Viewed from Pump Side, Sigma -Z

ORIGINAL PAGE
COLOR PHOTOGRAPH

ANSYS 4.3
APR 4 1989
15:06:24
POST1 STRESS
STEP=1
ITER=1
SIGE (AVG)

ZV=-1
DIST=3.72
XF=-.037
YF=-.0628
ZF=1.95
MX=80989
MN=31758
37225
42696
48167
53638
59109
64580
70051
75522
80989

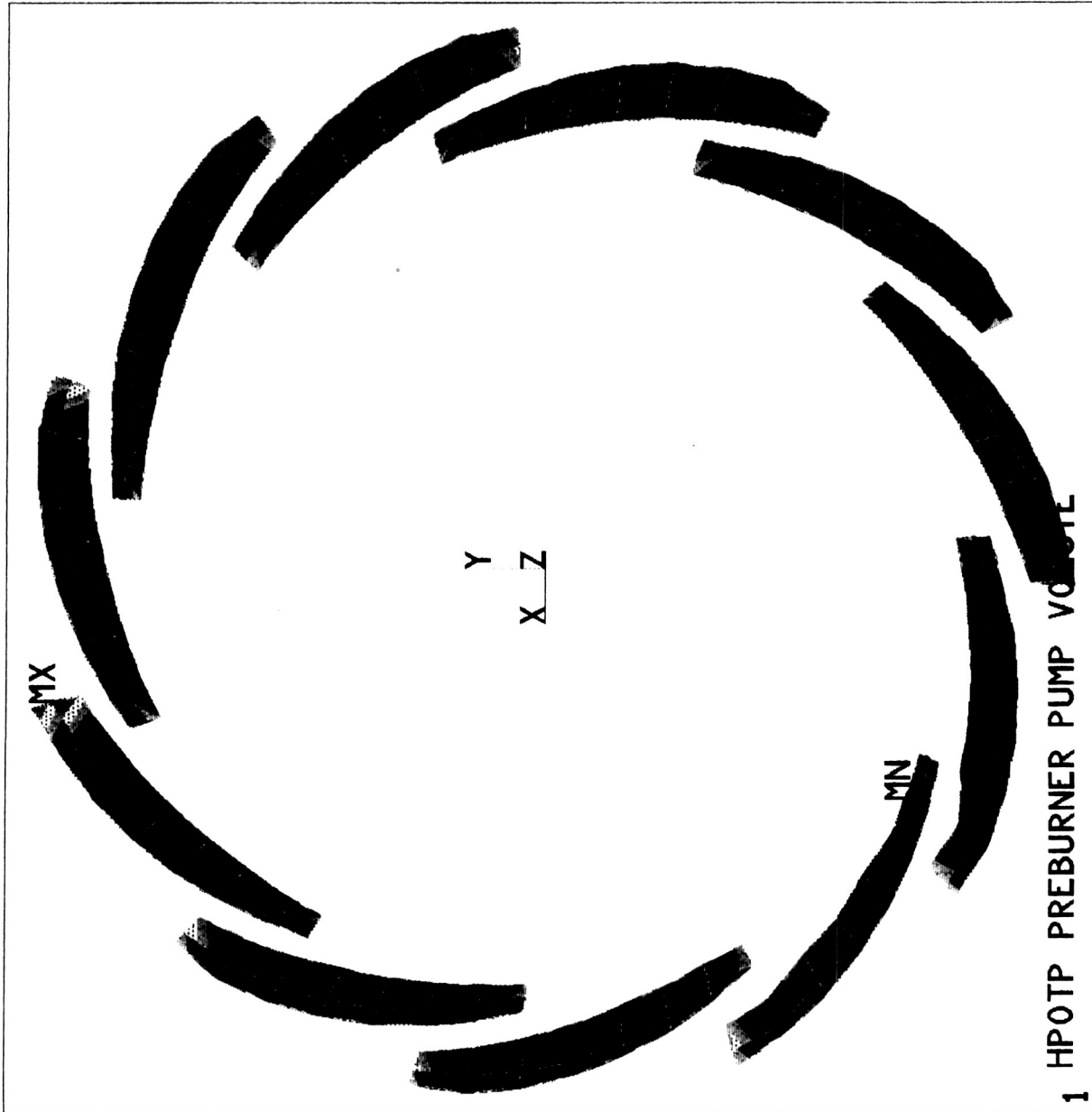


Figure 22 Vanes Viewed from Pump Side, Sigma -E

ORIGINAL PAGE
COLOR PHOTOGRAPH

ANSYS 4.3
APR 4 1989
10:08:52
POST1 STRESS
STEP=1
ITER=1
SIG1 (AVG)
DSYS=1

YV=1
DIST=2.23
XF=3.02
YF=3.89
ZF=2.08
ANGL=180
HIDDEN
MX=64823
MN=-3442
4143
11728
19313
26898
34483
42068
49653
57238
64823

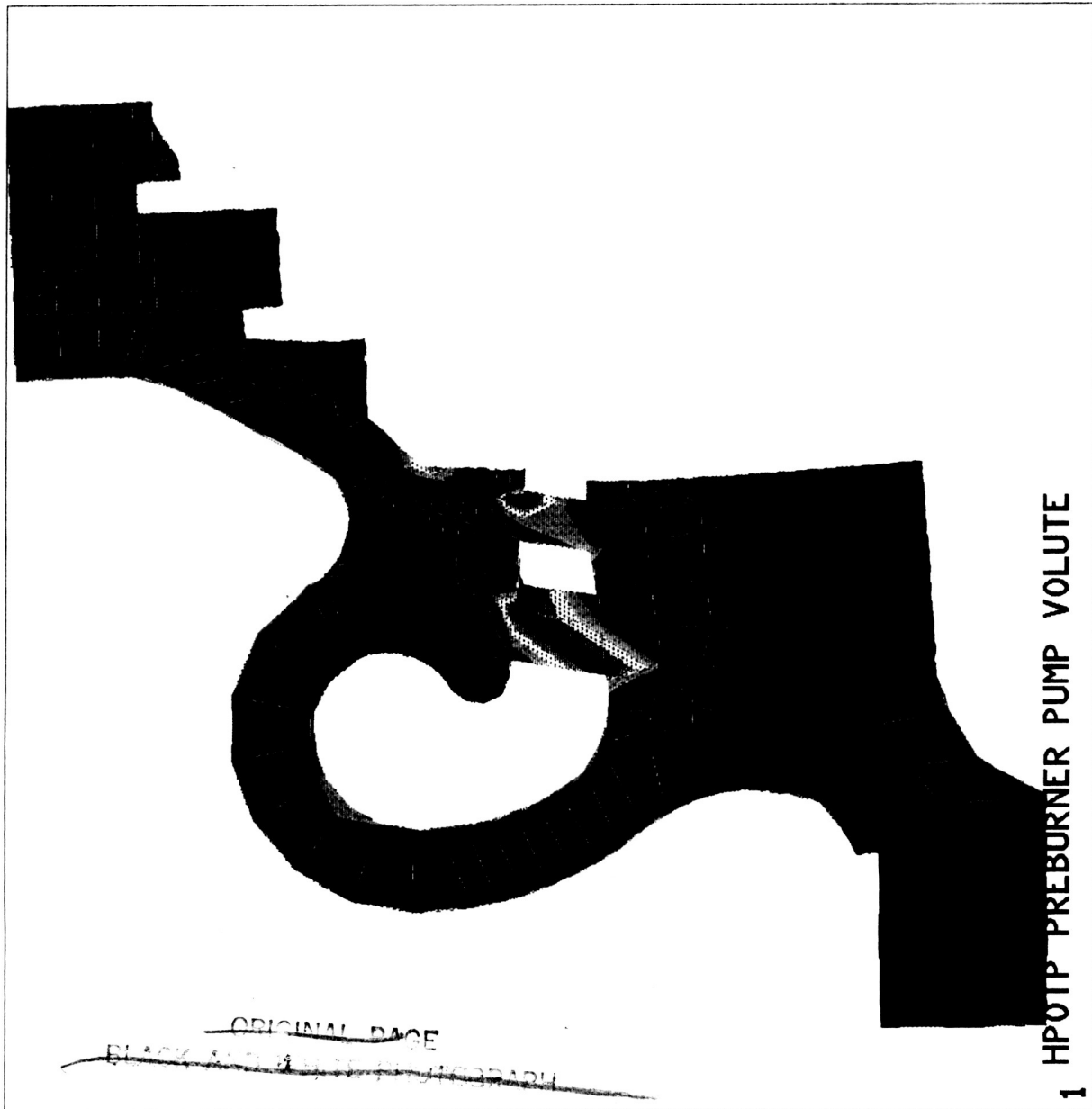


Figure 23 Sigma -1 for 68° to 76° Section

~~PRECEDING PAGE BLANK NOT FILMED~~

ORIGINAL PAGE
COLOR PHOTOGRAPH

ANSYS 4.3
APR 4 1989
10:21:24
POST1 STRESS
STEP=1
ITER=1
SIGE (AVG)
DSYS=1

YV=1
DIST=2.23
XF=3.02
YF=3.89
ZF=2.08
ANGL=180
HIDDEN
MX=67817
MN=1859
9187
16516
23845
31174
38503
45832
53161
60490
67817

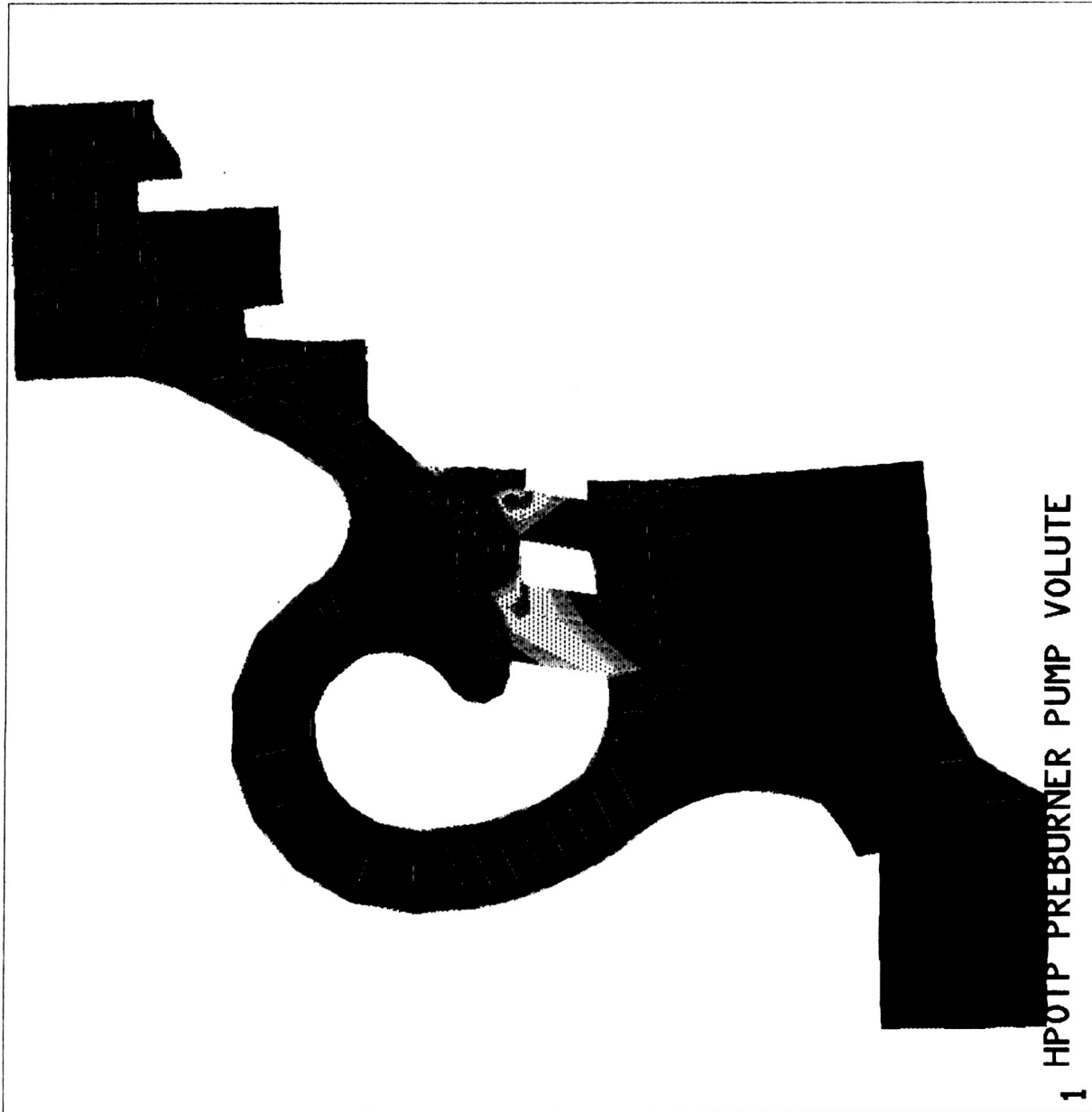


Figure 24 Sigma -E for 68° to 76° Section

ORIGINAL PAGE
COLOR PHOTOGRAPH

ANSYS 4.3
APR 4 1989
9:23:47
POST1 STRESS
STEP=1
ITER=1
SIG1 (AVG)
DSYS=1

YV=1
DIST=2.23
XF=3.02
YF=1.05
ZF=2.08
ANGL=180
HIDDEN
MX=60824
MN=-549
6267
13087
19907
26727
33547
40367
47187
54007
60824

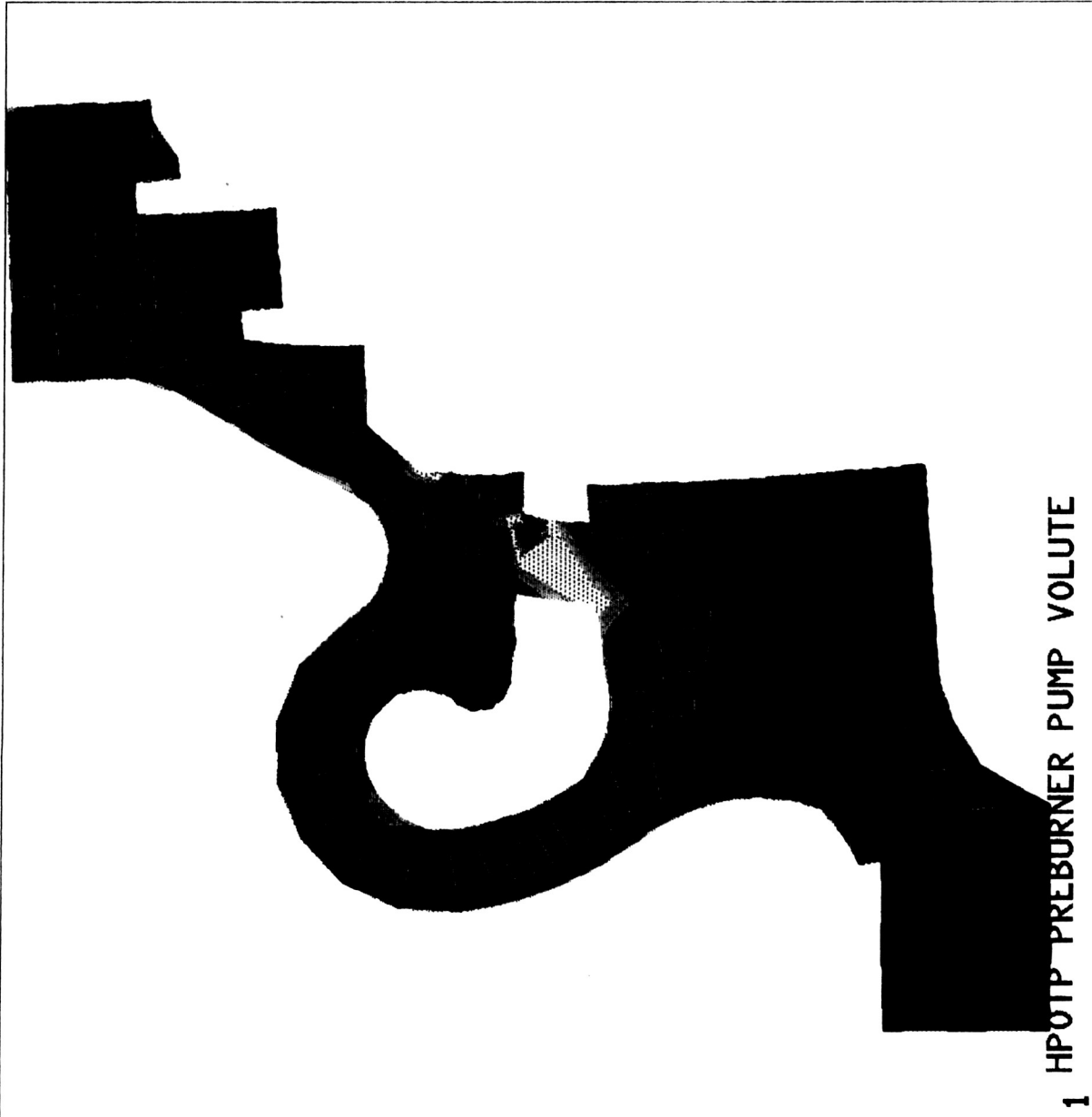


Figure 25 Sigma -1 for 14° to 22° Section

ANSYS 4.3
APR 4 1989
9:34:07
POST1 STRESS
STEP=1
ITER=1
SZ (AVG)
CSYS=1
DSYS=1

YV=1
DIST=2.23
XF=3.02
YF=1.05
ZF=2.08
ANGL=180
HIDDEN
MX=54739
MN=-17467
-9445
-1422
6601
14624
22647
30670
38693
46716
54739

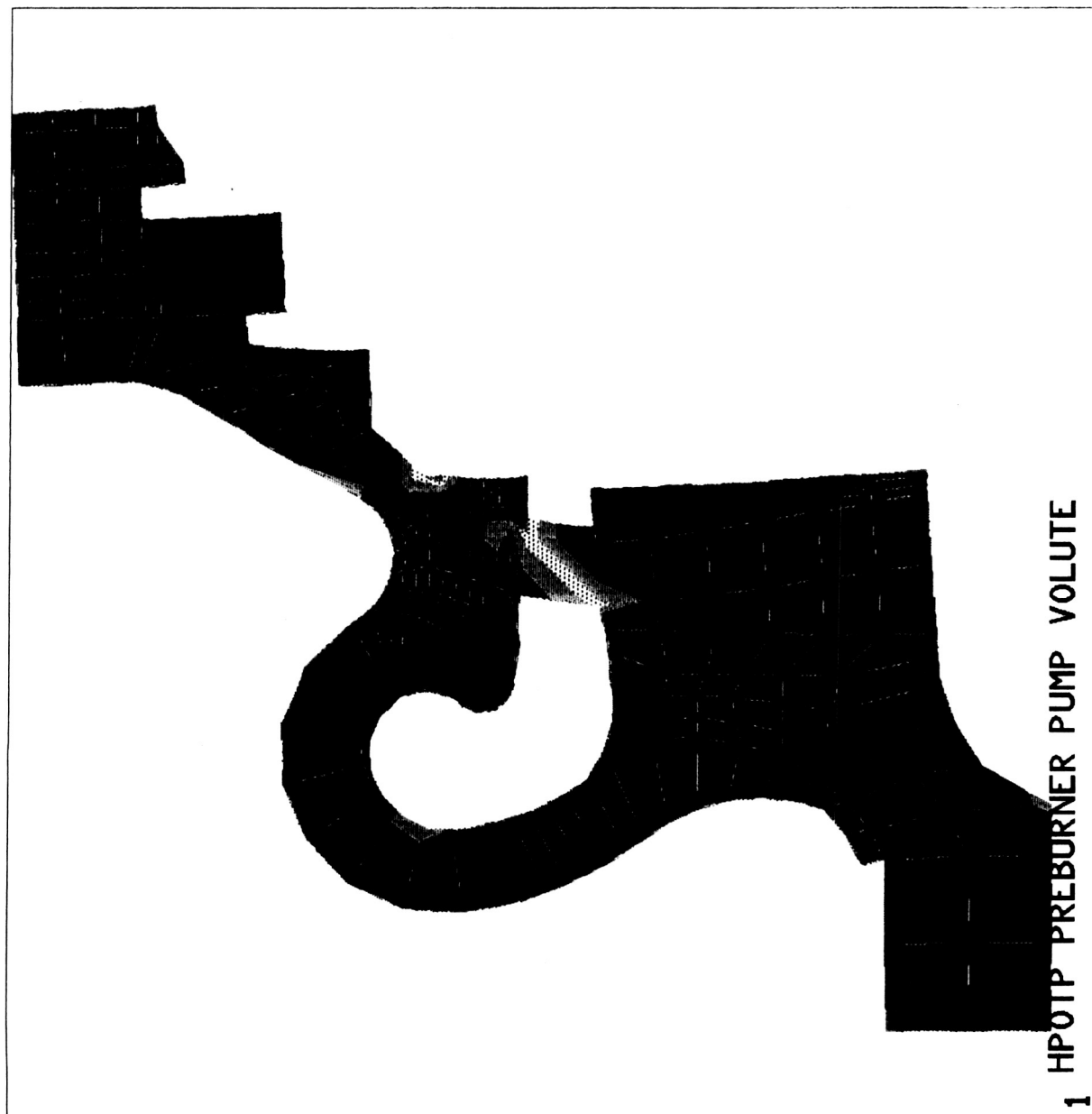


Figure 26 Sigma -Z for 14° to 22° Section

ORIGINAL PAGE
COLOR PHOTOGRAPH

ANSYS 4.3
APR 4 1989
9:46:59
POST1 STRESS
STEP=1
ITER=1
SIGE (AVG)
DSYS=1

YV=1
DIST=2.23
XF=3.02
YF=1.05
ZF=2.08
ANGL=180
HIDDEN
MX=55628
MN=1719
7708
13698
19688
25678
31668
37658
43648
49638
55628

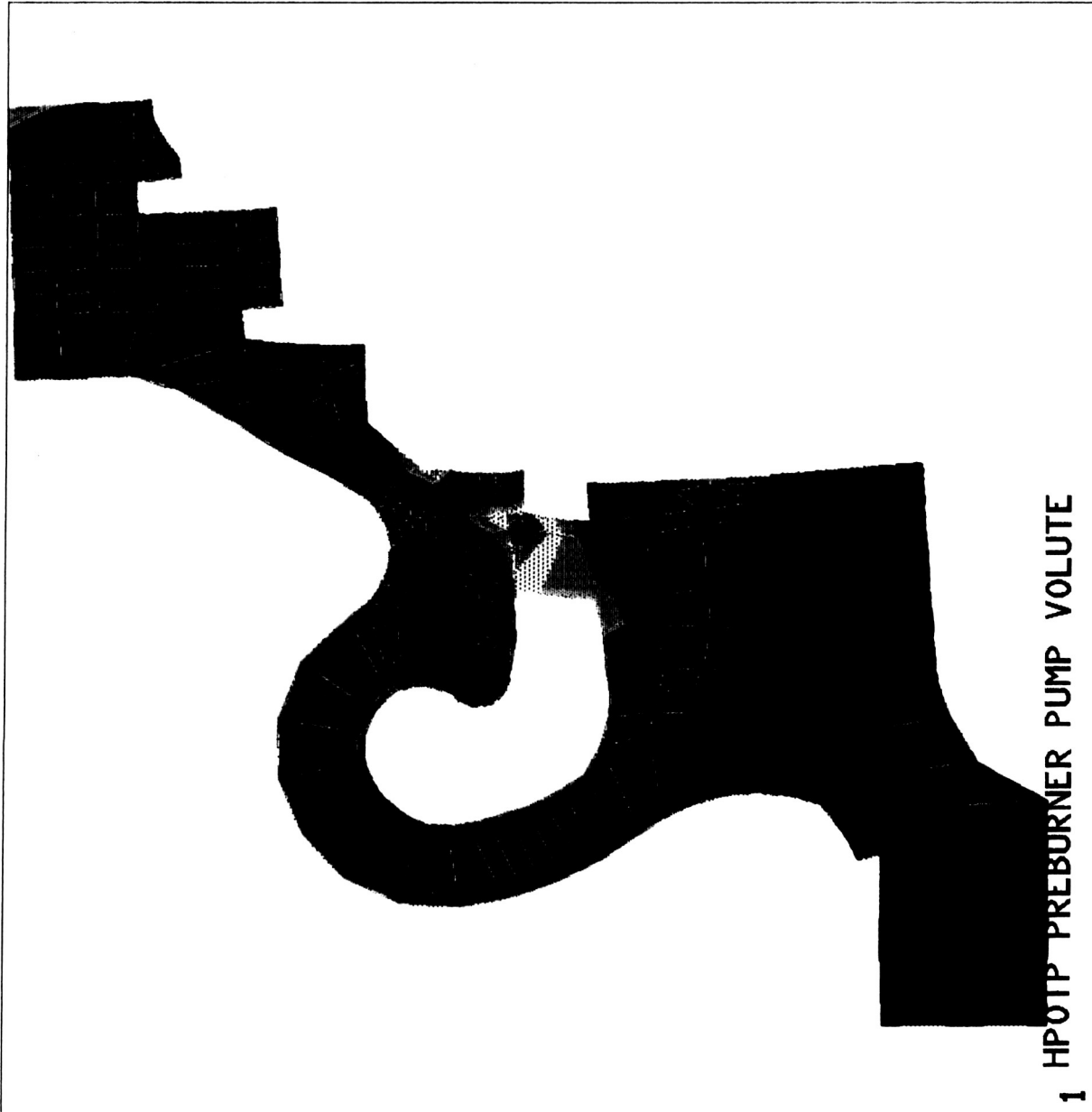


Figure 27 Sigma -E for 14° to 22° Section